



Universidade de Vigo

Trabajo Fin de Máster

Analysis of the stock-recruitment relationship for the southern horse mackerel (*Trachurus trachurus*) stock in the ICES Division 27.9.a. in preparation for Management Strategy Evaluation (MSE).

Helena Puente Rodríguez

Máster en Técnicas Estadísticas

Curso 2025-2026

Propuesta de Trabajo Fin de Máster

<p>Título en galego: Análise da relación stock-recrutamento para o stock de xurel do sur (<i>Trachurus trachurus</i>) na División 27.9.a do ICES, en preparación para a Avaliación de Estratexias de Xestión (MSE).</p>
<p>Título en español: Análisis de la relación stock-reclutamiento para el stock de jurel sur (<i>Trachurus trachurus</i>) en la División 27.9.a del ICES, en preparación para la Evaluación de Estrategias de Gestión (MSE).</p>
<p>English title: Analysis of the stock-recruitment relationship for the southern horse mackerel (<i>Trachurus trachurus</i>) stock in the ICES Division 27.9.a. in preparation for Management Strategy Evaluation (MSE).</p>
<p>Modalidad: Modalidad B</p>
<p>Autor/a: Helena Puente Rodríguez, Universidad de Santiago de Compostela</p>
<p>Director/a: Javier Roca Pardiñas, Universidad de Vigo</p>
<p>Tutor/a: Adriana Nogueira Gassent, IEO-CSIC; Gersom Costas Bastida, IEO-CSIC</p>
<p>Breve resumen del trabajo: Explore how different assumptions about the stock-recruitment (SR) relationship affect the performance of management strategies within a Management Strategy Evaluation (MSE) framework.</p>
<p>Recomendaciones:</p>
<p>Otras observaciones:</p>

Don/doña Javier Roca Pardiñas, catedrático de la Universidad de Vigo, don/doña Adriana Nogueira Gassent, Investigadora M3 de IEO-CSIC, y don/doña Gersom Costas Bastida, Técnico superior especializado de OPIS de IEO-CSIC, informan que el Trabajo Fin de Máster titulado

**Analysis of the stock-recruitment relationship for the southern horse mackerel
(*Trachurus trachurus*) stock in the ICES Division 27.9.a. in preparation for
Management Strategy Evaluation (MSE).**

fue realizado bajo su dirección por don/doña Helena Puente Rodríguez para el Máster en Técnicas Estadísticas. Estimando que el trabajo está terminado, dan su conformidad para su presentación y defensa ante un tribunal. Además, Don/doña Javier Roca Pardiñas y don/doña Helena Puente Rodríguez

sí no

autorizan a la publicación de la memoria en el repositorio de acceso público asociado al Máster en Técnicas Estadísticas.

En Vigo, a 3 de junio de 2026.

El/la director/a:

Don/doña Javier Roca Pardiñas

ROCA PARDIÑAS Firmado digitalmente por
ROCA PARDIÑAS JAVIER -
JAVIER - 77592181W
77592181W Fecha: 2026.06.03 12:15:34
+02'00'

El/la tutor/a:

Don/doña Gersom Costas Bastida

Firmado por COSTAS BASTIDA
GERSOM - DNI ***5070** el día
03/06/2026 con un certificado
emitido por AC Sector Público

El/la autor/a:

Don/doña Helena Puente Rodríguez



El/la tutor/a:

Don/doña Adriana Nogueira Gassent

NOGUEIRA
GASSENT
ADRIANA - DNI
14307098V

Firmado digitalmente por NOGUEIRA
GASSENT ADRIANA - DNI 14307098V
Nombre de reconocimiento (DN): c=ES,
o=CONSEJO SUPERIOR DE INVESTIGACIONES
CIENTÍFICAS, ou=CERTIFICADO
ELECTRÓNICO DE EMPLEADO PÚBLICO,
ou=CENTRO OCEANOGRÁFICO DE VIGO,
ou=14307098V,
serialNumber=DCES-14307098V,
sn=NOGUEIRA GASSENT,
givenName=ADRIANA, cn=NOGUEIRA
GASSENT ADRIANA - DNI 14307098V
Fecha: 2026.06.03 15:12:56 +02'00'

Declaración responsable. Para dar cumplimiento a la Ley 3/2022, de 24 de febrero, de convivencia universitaria, referente al plagio en el Trabajo Fin de Máster (Artículo 11, [Disposición 2978 del BOE núm. 48 de 2022](#)), **el/la autor/a declara** que el Trabajo Fin de Máster presentado es un documento original en el que se han tenido en cuenta las siguientes consideraciones relativas al uso de material de apoyo desarrollado por otros/as autores/as:

- Todas las fuentes usadas para la elaboración de este trabajo han sido citadas convenientemente (libros, artículos, apuntes de profesorado, páginas web, programas, ...)
- Cualquier contenido copiado o traducido textualmente se ha puesto entre comillas, citando su procedencia.

- Se ha hecho constar explícitamente cuando un capítulo, sección, demostración, . . . sea una adaptación casi literal de alguna fuente existente.

Y, acepta que, si se demostrara lo contrario, se le apliquen las medidas disciplinarias que correspondan.

Agradecimientos

I would like to express my deepest gratitude to all those who have accompanied me throughout this journey, without whom the completion of this work would not have been possible.

To my supervisors at the IEO, Adriana and Gersom, for their willingness to teach me, as well as for their commitment and patience in guiding me. I would also like to express my sincere gratitude to Hugo Mendes (IPMA) for his valuable contributions, insightful discussions, and generosity in sharing his knowledge throughout the development of this work.

To my parents and my sister, for their unconditional love and their support throughout my entire academic journey.

To my partner, who has always been there to support me with care and affection.

Thank you all.

I would like to thank the participants of the ICES Working Group on Southern horse mackerel, anchovy and sardine (WGHANSA) meeting, held from 25-28 May 2026, for their positive reception of my work. Sharing and discussing my research progress with such an experienced and knowledgeable group was a very enriching experience.

Contents

Resumen	xi
Preface	xiii
1 Introduction	1
2 Material and methodology	5
2.1 Study area	5
2.2 Data	5
2.2.1 Assessment model	6
2.2.2 Exploratory analysis and diagnostics	6
2.3 Stock-Recruitment models	8
2.3.1 Beverton and Holt's model	9
2.3.2 Beverton-Holt's model with autoregressive component	10
2.3.3 Ricker's model	10
2.3.4 Segmented regression model or Hockey-Stick	11
2.4 Uncertainty estimation using residual bootstrap	12
2.5 Stochastic simulation for Biological Reference Points	13
2.5.1 Biological Reference Points	14
2.5.2 Biological Reference Points: a deterministic approach	15
2.6 Sensitivity analysis	19
2.6.1 Steepness	19
2.6.2 Virgin recruitment	19
2.6.3 Density-dependent effects	20
2.7 Software used	21
3 Results	23
3.1 Exploratory analysis	23
3.2 Comparative evaluation of stock-recruitment models	27
3.2.1 Beverton-Holt model	27
3.2.2 Ricker model	29
3.2.3 Hockey-Stick model	31
3.2.4 Beverton-Holt model with an autoregressive component	33
3.2.5 Model comparison using AIC and BIC	36
3.3 Uncertainty estimation using residual bootstrap	37
3.4 Analysis of the S-R relationship under different productivity regimes	40
3.5 Biological Reference Points	42
3.6 Sensitivity analysis	44
3.6.1 Steepness	44
3.6.2 Virgin recruitment	45
3.6.3 Density-dependent effects	45

3.6.4	Calculus of the reference points using an alternative steepness	47
4	Discussion	49
5	Conclusions	53
	Glossary	69
	Bibliography	71

Resumen

Resumen en español

La relación stock-reclutamiento es uno de los procesos con mayor incertidumbre asociada en la dinámica poblacional de los peces. La evaluación del jurel del sur (*Trachurus trachurus*) en la División 9.a del ICES se realiza mediante el modelo integrado de evaluación de stocks Stock Synthesis III (SS3) desde 2024. Sin embargo, cuando se implementó el modelo, la relación stock-reclutamiento (SRR, por sus siglas en inglés) y los parámetros asociados no fueron revisados. En este trabajo utilizamos los resultados de la evaluación de este stock para revisar la SRR. Para ello, exploramos diferentes modelos de relación stock-reclutamiento (Beverton-Holt, Ricker y Hockey-Stick), cuantificamos la incertidumbre asociada a estos modelos, analizamos la sensibilidad de los parámetros y estimamos puntos biológicos de referencia incorporando explícitamente dicha incertidumbre. Los resultados obtenidos están destinados a mejorar la configuración del modelo de evaluación del stock y a contribuir al desarrollo de modelos operativos robustos que posteriormente puedan aplicarse dentro de un marco de Evaluación de Estrategias de Gestión (Management Strategy Evaluation, MSE) para la gestión del jurel.

Resumo en galego

A relación stock-recrutamento é un dos procesos con maior incerteza asociada na dinámica poboacional dos peixes. A avaliación do xurelo do sur (*Trachurus trachurus*) na División 9.a do ICES realízase mediante o modelo integrado de avaliación de stocks Stock Synthesis III (SS3) desde 2024. Porén, cando se implementou o modelo, a relación stock-recrutamento (SRR, polas súas siglas en inglés) e os parámetros asociados non foron revisados. Neste traballo utilizamos os resultados da avaliación deste stock para revisar a SRR. Para iso, exploramos diferentes modelos de relación stock-recrutamento (Beverton-Holt, Ricker e Hockey-Stick), cuantificamos a incerteza asociada a estes modelos, analizamos a sensibilidade dos parámetros e estimamos puntos biolóxicos de referencia incorporando explícitamente dita incerteza. Os resultados obtidos están destinados a mellorar a configuración do modelo de avaliación do stock e a contribuír ao desenvolvemento de modelos operativos robustos que posteriormente poidan aplicarse dentro dun marco de Avaliación de Estratexias de Xestión (Management Strategy Evaluation, MSE) para a xestión do xurelo.

English abstract

Stock-recruitment relationship is one of the most uncertain processes in fish population dynamics. The horse mackerel (*Trachurus trachurus*) in ICES Division 9.a assessment has been conducted using the integrated stock assessment model Stock Synthesis III (SS3) since 2024. However, when the model was implemented, the stock-recruitment relationship (SRR) and its associated parameters were not revised. Here we use the outputs from the assessment this stock to revise the SRR. For that, we explored different SR models (B-H, Ricker and Hockey-Stick), quantified the uncertainty associated with these models, analysed parameter sensitivity and estimated biological reference points while explicitly

accounting for uncertainty. The results obtained are intended to improve the model configuration of the stock assessment model and to contribute to the development of robust operating models that can subsequently be applied within a MSE framework for horse mackerel management.

Preface

Aquatic ecosystems are characterized by a high level of diversity that provides a wide range of environmental, economic, and social benefits. At the global level, there is increasing recognition of their nutritional value and of the ecosystem services they provide for maintaining healthy diets and preserving biodiversity. Consequently, these systems represent strategic solutions for improving food security, supporting livelihoods, and achieving the objectives of the 2030 Agenda for Sustainable Development, particularly in combating hunger, malnutrition, and poverty in coastal and riparian communities (FAO, 2024).

Reflecting their increasing importance, global fisheries and aquaculture production reached a historic record of 223.2 million tonnes in 2022, a 4% increase compared with 2020 (FAO, 2024). This continued growth highlights both the opportunities and the need to promote management and development pathways that ensure the expansion of aquatic food systems remains equitable, resilient, and environmentally sustainable.

Historically, the governance of marine common goods was guided by the principle of the “freedom of the seas”, based on the belief that resources were limited yet renewable. However, the expansion of fishing activity and technological advances in the 19th and 20th centuries revealed the finite nature of these ecosystems. This realization prompted a transition from open-access exploitation to more strict regulation. A foundational milestone in this process was the 1982 United Nations Convention on the Law of the Sea (UNCLOS), which established the Exclusive Economic Zone (EEZ) (UNCLOS, 1982). This extended the jurisdiction of coastal states to 200 nautical miles (Russ, 2003), effectively ending the open-access regime in coastal areas and granting nations not only sovereign rights over resources but also the legal responsibility to conserve and manage them wisely (Nogueira, 2017).

Despite the legal progress made in 1982, fishing pressure continued to exceed the regenerative capacity of many species. The 1980s marked a turning point with the collapse of fisheries such as the Newfoundland cod fishery (*Gadus morhua*) (Rose, 2003). This biological and socio-economic crisis demonstrated that even the most abundant populations are vulnerable under poor management (Myers, 1997), forcing the international community to define sustainable fishing not only as an economic objective but as a biological imperative (Walters, 1996).

In response to scientific uncertainty, the Food and Agriculture Organization of the United Nations (FAO) adopted the Precautionary Approach (PA) in 1995 through the Code of Conduct for Responsible Fisheries (FAO, 1995). This principle establishes that a lack of scientific information should not be taken as a reason to postpone the adoption of conservation measures. Subsequently, at the Johannesburg Summit in 2002 (UN, 2002) a commitment was reached to achieve the Maximum Sustainable Yield (*MSY*) which was defined as the highest catch that can be taken from a population indefinitely without compromising its future productivity.

The practical implementation of fisheries assessment and management frameworks requires robust scientific evidence, long-term monitoring programs, and strong marine research infrastructure. In the Northeast Atlantic, a central role in coordinating and providing this scientific basis is played by the International Council for the Exploration of the Sea (ICES) (Figure 1). Established in 1902, ICES is an intergovernmental organization that coordinates marine research and provides independent scientific advice to governments and regional fisheries management bodies. Through a network of expert working groups, ICES evaluates the status of fish stocks, develops assessment methodologies, and delivers advice

that supports the sustainable management of marine resources in accordance with the PA and MSY objectives (<https://www.ices.dk/Pages/default.aspx>).

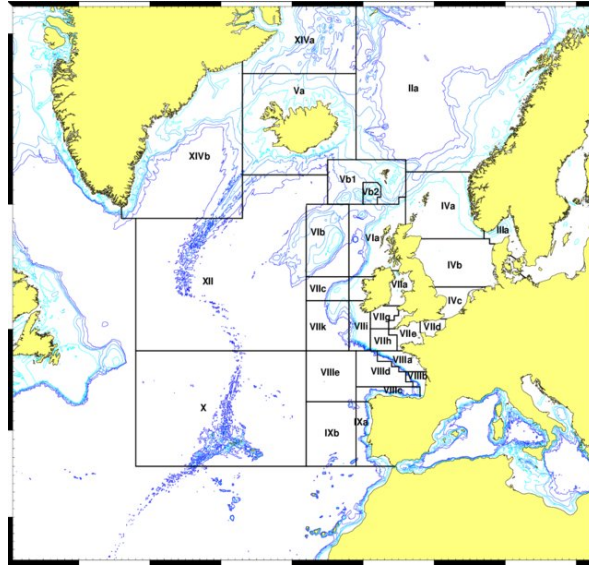


Figure 1: Map of ICES' Sub-areas and divisions in the North East Atlantic.

The practical implementation of the assessment and fisheries management models requires robust scientific and marine research infrastructure.

The IEO-CSIC is a leading marine research institution dedicated to advancing scientific knowledge of the oceans, promoting the sustainable management of fishery resources, and improving understanding of the marine environment. As Spain's principal public institution for marine science and fisheries research, the IEO-CSIC provides scientific advice to the Spanish Government on the status of fishery resources of interest to the Spanish commercial fishing fleet and represents Spain in international fisheries management organizations. (<https://www.ieo.es/es/>).

In this context, the present Master's thesis has been developed under the supervision of researchers from the Instituto Español de Oceanografía del Consejo Superior de Investigaciones Científicas (IEO-CSIC), through an internship agreement. This work has been developed within the framework of the work carried out by the IEO-CSIC, Centro Oceanográfico de Vigo (COV) in its pursuit of solutions for the sustainable management of fisheries resources, and has been developed within the ICES Fisheries Programme and the Methods in Ecology and Assessment of Living Marine Resources research group (METMAR).

Chapter 1

Introduction

The sustainable management of fisheries resources is a fundamental challenge not only from an ecological perspective because of the need to preserve marine ecosystems, but also from an economic and social perspective, as fisheries contribute significantly to food security and market demands. Fisheries exploitation therefore requires continuous and rigorous assessments that take multiple factors into account to ensure that fishing rates are sustainable in the long term. For this purpose, mathematical and statistical models are used to integrate catch data and scientific survey information in order to reconstruct fish population dynamics.

Stock Assessment is the statistical and biological process through which the status of a fish population or stock and its response to fishing pressure are estimated (Hilborn and Walters, 1992). It fundamentally involves two essential tasks: estimating the historical and current abundance of resources, and projecting their future evolution. Its main objective is to provide scientific advice for the sustainable management of marine resources, allowing determination of harvest levels that do not compromise the long-term viability of fish populations.

The accuracy of an assessment depends on the quality and availability of input data, which generally come from three sources: fishery dependent data derived from the fishing process itself data (catch data, providing information on total removals by the fishing fleet; fishery independent data derived from research surveys (indices estimates); and biological data, such as size, age, and maturity samples, obtained from both commercial fisheries and scientific surveys.

However, despite the increasing quantity and quality of available information, stock assessments remain subject to multiple sources of uncertainty that can affect estimates of stock status and management advice. These uncertainties arise from limitations in the data, natural variability in population dynamics and environmental conditions, and assumptions made within assessment models. Consequently, fisheries science increasingly focuses on quantifying and incorporating uncertainty into the assessment process in order to improve the robustness and reliability of management recommendations (Punt and Hilborn, 1997).

In this context, dynamic models are fundamental tools in stock assessment because they describe how fish populations change over time in response to biological processes and fishing pressure. These models integrate information on growth, recruitment, natural mortality, and exploitation to reconstruct past population trajectories and predict future stock dynamics under different management scenarios. Depending on the available data and the complexity required, dynamic models can range from simple biomass production models to age- or size-structured and fully integrated assessment frameworks. Their main objective is to provide a quantitative basis for understanding population status and supporting sustainable fisheries management.

Three main types of models can be distinguished:

- Global models (or surplus production models): These are the simplest and do not require information on population structure (age or size), as they treat the stock as a single biomass unit.

They are based on the idea that surplus production is maximized at intermediate levels of abundance. They are particularly useful to estimate MSY when only time series of catch and effort are available (Scheafer, 1954; Cousido-Rocha et al., 2022).

- Age- (or size-) structured models: These models analyze population dynamics by tracking each cohort (i.e., individuals born in the same year) over time. They recognize that mortality, growth, and reproductive potential vary significantly with age. Techniques such as Virtual Population Analysis (VPA) are used to reconstruct historical stock abundance and to understand how fishing selectively affects juveniles or adults (Pope, 1972; Skalski et al., 2010).
- Integrated models: These represent the most advanced standard in contemporary fisheries assessment, with Stock Synthesis (SS3) (Methot and Wetzel, 2013) being a prominent example. They simultaneously combine all relevant sources of information (catches, CPUE, age data, tagging data, and environmental variables) within a single statistical framework, typically based on maximum likelihood or Bayesian approaches. Their main advantage lies in their ability to account for uncertainty and to simulate complex ecological (Maunder and Punt, 2013) processes.

A fundamental concept in fisheries research is the “stock”, which is defined as a population of fish of a given species that inhabits a delimited geographical area and functions as a management or exploitation unit for that species. These individuals exhibit biological parameters that are sufficiently homogeneous and isolated from other groups to be modeled independently (Begg et al., 1999).

Determining the status of a stock involves estimating biological parameters, such as abundance (number of fish) or biomass (weight), and comparing these estimated values with certain reference values that define desirable conditions, Biological Reference Points (BRPs), which represent precautionary thresholds for stock conservation and exploitation. Among these, MSY is one of the most widely used concepts. ICES defines MSY as the maximum long-term average yield that can be taken from a stock while maintaining its productivity (ICES, 2023). The associated fishing mortality, $FMSY$, represents the exploitation rate expected to produce MSY under equilibrium conditions and therefore constitutes a central target in fisheries management.

Two important indicators used in fisheries management are stock biomass and fishing mortality. Stock biomass is the total weight of all individuals composing the stock, while Spawning Stock Biomass (SSB) refers specifically to the biomass of mature individuals capable of contributing to reproduction. Estimates of current biomass are compared with BRPs assumed to be sufficient to produce an adequate number of juveniles in the following spawning period. Maintaining biomass above these reference values is synonymous with stock sustainability; whereas biomass falling below them indicates that the population is overexploited. Fishing mortality (F) defined as the instantaneous rate at which individuals are removed due to fishing activity, is another key indicator. Similarly, when fishing mortality exceeds a sustainable level, the stock is considered to be undergoing overfishing.

Forecasts and projections are essential components of management programs because they allow the evaluation of future catch scenarios, recovery strategies, and conservation measures (Kilduff et al., 2009). One of the most important and challenging aspects of these projections is the stock-recruitment relationship, which describes how SSB influences the number of recruits entering the population each year (Hilborn and Walters, 1992; Kilduff et al., 2009). To understand this relationship, two fundamental pillars of fisheries ecology are introduced.

SSB is the total weight of all individuals in the population that have reached sexual maturity and are therefore capable of contributing to reproduction in a given year. Recruitment (R) is the number of new individuals that survive and enter the assessed population or fishery each year, also referred to as recruits. The stock-recruitment (S-R) relationship is therefore fundamental for understanding population productivity, resilience, and the capacity of a stock to respond to exploitation and environmental variability.

Because the S-R relationship plays a central role in projecting future population dynamics, it also constitutes a key component of Management Strategy Evaluation (MSE). MSE frameworks use simulation approaches to test the performance of alternative management strategies under different

sources of uncertainty, including variability in recruitment, observation error, and implementation error. In this context, the S-R relationship is incorporated into operating models to simulate future stock trajectories and evaluate the robustness of harvest control rules and management procedures.

The Atlantic horse mackerel (*Trachurus trachurus*) is a teleost fish belonging to the order Perciformes and the family Carangidae (Figure 1.1). It is a pelagic species inhabiting depths from the surface down to 500 meters, although it is more frequently found within the 100 to 200-meter stratum (FAO- FIGIS, 2005). Its geographical distribution is extensive, spanning the Eastern Atlantic from Norway to the Cape of Good Hope (South Africa), with incursions into the southwestern Indian Ocean and a significant presence in the Baltic, North, Mediterranean, and Black Seas. Adults generally aggregate in large schools, particularly in coastal and continental shelf areas over sandy bottoms.



Figure 1.1: Southern horse mackerel (*Trachurus trachurus*).

Horse mackerel is managed as three different stocks in the Northeast Atlantic: Western stock, Northsea stock and Southern stock (Figure 1.2). Here I will focus on the Southern stock, ICES Division 9a (ICES, 2025). The historical Spanish and Portuguese catches from 1992, as seen in Figure 1.3, exhibits fluctuant dynamics, with an average oscillating near 25,000 tonnes.

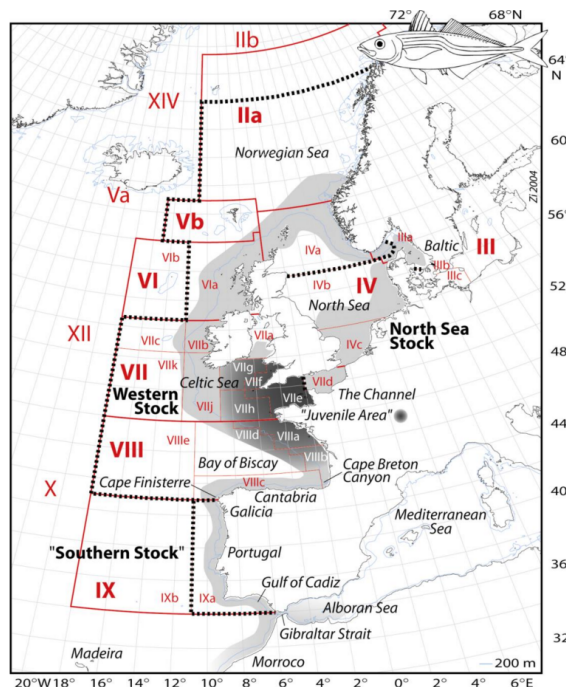


Figure 1.2: Stocks of horse mackerel and distribution across the Northeast Atlantic.

The annual assessment of the status and population dynamics of small pelagic stocks in Southern

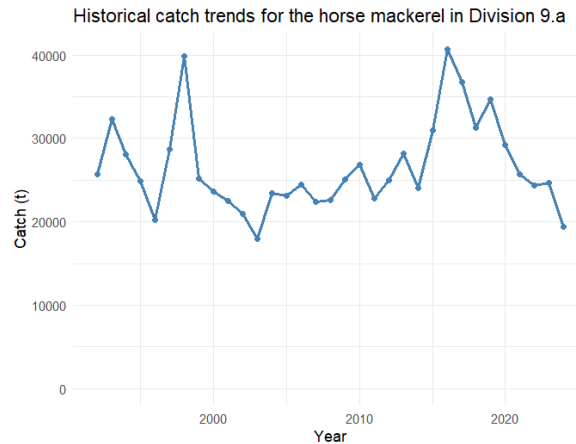


Figure 1.3: Catch trends for the Southern horse mackerel in ICES Division 9a.

European Atlantic waters (corresponding to Divisions 9.a and 8.c) is conducted by the WGHANSA (Working Group on Southern Horse Mackerel, Anchovy, and Sardine) which is a specialized technical body within the ICES. By synthesizing data from commercial fishery landings and independent scientific surveys, WGHANSA provides the rigorous scientific advice required by international management bodies to determine Total Allowable Catches (TACs) and ensure the long-term biological and economic sustainability of these resources (ICES, 2025). To provide this advice, stock assessments estimate key population parameters, including stock abundance, fishing mortality, and BRPs, which are used to evaluate stock status and define management targets.

Since 2024, the assessment of the Southern horse mackerel has been conducted using the integrated stock assessment model Stock Synthesis III (SS3) (ICES, 2025). However, although the assessment model was updated, the S-R relationship and its associated parameters were retained from previous assessments and have not been comprehensively re-evaluated. Given the central role of the S-R relationship in determining stock productivity, estimating recruitment, and BRPs revisiting this relationship is essential to ensure that management advice is based on the best available scientific evidence.

The main objective of this thesis is to review the S-R relationship for Southern horse mackerel in ICES Division 9a. For that, I explored different models for the S-R relationship, quantified the uncertainty associated with these models, analysed parameter sensitivity and estimated BRPs while explicitly accounting for uncertainty. The results obtained are intended to improve the settings of the stock assessment use to manage the stock, and to propose new BRPs. Furthermore, the results could contribute to the development of robust operating models for future application in the development of MSE framework, strengthening the scientific basis for the long-term management of this stock.

Chapter 2

Material and methodology

2.1 Study area

The southern stock population of horse mackerel exhibits a geographic distribution spanning the Western Atlantic coastline of the Iberian Peninsula, from the Strait of Gibraltar to Cape Finisterre in Galician waters in the northwestern region of Spain (Mendes et al., 2024). That corresponds to the division 9a in ICES (Figure 2.1).



Figure 2.1: Statistical subdivisions within ICES Division 9.a.

2.2 Data

The horse mackerel assessment was conducted using the integrated stock assessment Stock Synthesis III (SS3) (Methot and Wetzel, 2013). The data used for the analysis are the time-series (1992-2024) of *SSB* and recruitment taken from the most recent assessment conducted by Hugo Mendes (WGHANSA, 2024).

2.2.1 Assessment model

The SS3 model (Methot and Wetzel, 2013) is an integrated statistical and biological framework designed to incorporate multiple data sources and biological processes into a single coherent structure. Unlike traditional surplus production models, SS3 is an age-structured model distinguished by its scalability, allowing it to operate in data-limited contexts (functioning as an age-structured production model) as well as in highly complex assessments involving multiple fleets, geographic areas, and environmental processes.

The core of this system is divided into three fundamental components. The population submodel defines the biological dynamics, including recruitment, growth, and mortality, and allows for the modeling of temporal variability in these processes. The observation submodel generates expected values for observed data, such as abundance indices or size and age compositions, based on selectivity and population structure. Finally, the statistical estimation component uses maximum likelihood or Bayesian methods to minimize the difference between observed and expected data, providing robust estimates of uncertainty (Methot and Wetzel, 2013).

Given the intrinsic complexity of integrated models, the risk of misspecification is high. Therefore, rigorous evaluation is required based on four plausibility criteria: convergence, goodness-of-fit, consistency, and predictive capacity (Carvalho et al., 2021), using diagnostic tools such as residual analysis, likelihood profiles, or cross-validation. One of the most significant contributions of this framework is its ability to manage uncertainty in fisheries management. By incorporating recruitment functions (such as Beverton-Holt or Ricker) and allowing nearly any parameter to vary over time, the model facilitates the development of scientifically grounded projections.

Figures 2.2 and 2.3 show the time series corresponding to SSB and recruitment output estimates, respectively.

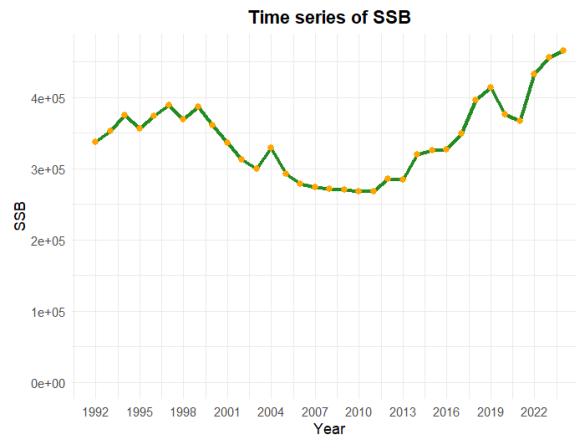


Figure 2.2: Time series of SSB levels between 1992 and 2024.

The assessment model applied to southern horse mackerel follows the configuration described in ICES (2025). In Annex A, Table 1 summarizes the main structural assumptions, input data, and parameter settings used in the assessment. In Figure 2.4, the SSB , Recruitment and F estimates (with confidence intervals) from the outputs of SS3 are shown.

2.2.2 Exploratory analysis and diagnostics

To characterize the relationship between SSB and R , a multi-model statistical approach was implemented using the R environment (R Team, 2026). First, an exploratory data analysis was conducted through the generation of pairs plots and correlation matrices to visualize the joint distribution of variables, their marginal densities, and potential skewness. The independence of recruitment events

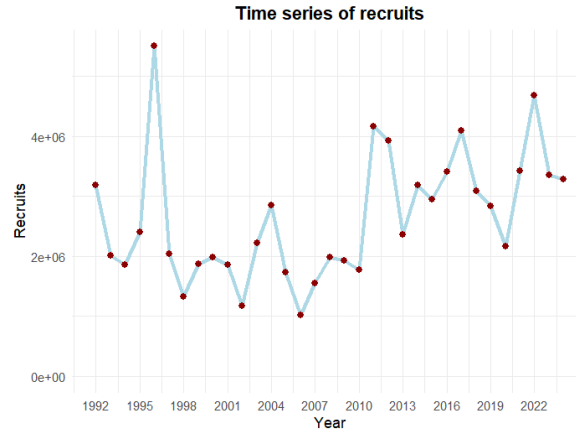


Figure 2.3: Time series of recruitment levels between 1992 and 2024.

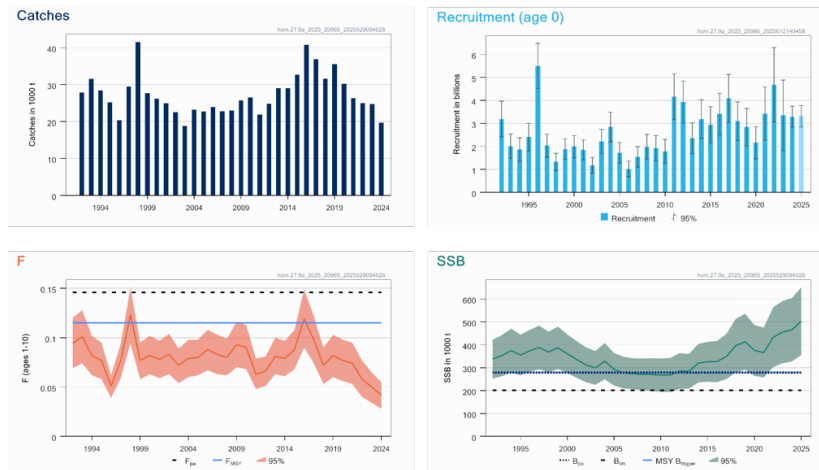


Figure 2.4: Caption

over time was assessed using the Autocorrelation Function (ACF) to detect any significant temporal lag effects. In this study, the analyses performed follow a methodology similar to the one described by Yang and Yamakawa (2022).

The functional relationship was modeled using three distinct approaches, a Simple Linear Regression (SLR) was fitted to both the original and log-transformed data to evaluate the baseline connectivity between SSB and R ; then a Generalized Additive Model (GAM) with smoothing splines was employed to account for potential non-linearities without assuming a rigid functional form. The complexity of this fit was determined by the Effective Degrees of Freedom (EDF). Then classical fisheries models, such as the Beverton-Holt, Ricker, and Segmented Regression (Hockey-Stick), were fitted to the data to derive biologically meaningful parameters (a and b).

The robustness and validity of these models were evaluated through a comprehensive suite of diagnostic tools. The goodness-of-fit was assessed via the coefficient of determination (R^2) and the Akaike Information Criterion (AIC) and Bayesian Information Criterion (BIC). The residual analysis, such as examination of normality (QQ-plots) and homoscedasticity (residuals vs. fitted values) and influence analysis to identify outliers and influential years using Cook's distance.

Finally, to address the observation of different productivity regimes, the dataset was partitioned into two periods (1992-2010 and 2010-2024). Year 2010 was included in both periods for convergence

reasons. A comparative analysis using boxplots and separate parametrizations was performed to test the hypothesis of a shift in the stock's reproductive efficiency.

Using the Wilcoxon-Mann-Whitney statistical test, I assessed whether the distribution of data after 2010 is greater or smaller than that of the previous years. Therefore, let $X = \text{Recruitment from Period 1 (1992-2010)}$, with size n_1 and $Y = \text{Recruitment from Period 2 (2010-2024)}$, with size n_2 . The test evaluates whether the probability that a randomly selected value from one period exceeds that from the other is 50%, considering the following null hypothesis:

$$H_0 : P(X > Y) = P(Y > X) = 0.5$$

against

$$H_1 : P(X > Y) \neq 0.5.$$

2.3 Stock-Recruitment models

Several mathematical formulations have been proposed to describe the relationship between spawning stock size and recruitment. Here I selected the most commonly applied in fisheries (Beverton and Holt, Ricker, and segmented regression), along with their mathematical formulations and underlying assumptions. It is important to emphasize that the relationship between stock size and resulting recruitment is non-deterministic and may involve various forms of feedback. It is in fact, one of the most uncertain processes of fish population dynamics, and is highly influential with respect to fisheries management advice (Maunder, 2012).

The analysis of the S-R relationship consists of examining the empirical relationship between SSB and the subsequent recruitment of the year class produced by that spawning event. This analysis was most commonly performed by fitting various curves to the data, with the resulting curve referred to as the S-R relationship.

As mentioned previously, recruitment is defined as the capacity of a population to produce a cohort of new individuals that enter the population and ensure its sustainability. In the context of population dynamics, a cohort refers to the group of individuals of the same species and approximately the same age that belong to a given population.

It is therefore logical to study the type of relationship that exists between the number of reproductively active individuals of a species and their ability to produce a cohort that will join the population and ensure the continuity of the species. This relationship is known as the stock-recruitment (SR) relationship, which has been extensively studied by numerous authors, such as Hilborn and Walters (1992) or Myers (2001). As previously noted, these relationships are non-deterministic and exhibit a high degree of uncertainty, often driven by external environmental factors, as said in Yang and Yamakawa (2022). However, as more effective techniques for measuring stock size and resulting recruitment have been developed, S-R relationships have become more precise, as noted in Hilborn and Walters (1992).

Ricker (1975) discussed the desirable properties of stock-recruitment curves and identified four basic properties to consider:

- A stock-recruitment curve must pass through the origin; when there is no parental stock, there is no recruitment.
- The curve should not decline to the horizontal axis at high stock levels, so that reproduction is not completely eliminated at high densities.
- The recruitment rate (recruits per spawner) should decrease continuously as parental stock increases.
- Recruitment should exceed parental stock over some range of possible parental stock values.

Hilborn and Walters (1992) also presented two additional properties related to the adequate fitting of S-R relationships: continuity (assuming that average recruitment varies smoothly) and stationarity (the relationship does not change significantly over time).

In the fisheries literature, S-R models can be classified as parametric, semi-parametric, or non-parametric. I mostly focused on the parametric approach, where I highlighted the classical models. This includes two-parameter models: the Beverton and Holt (1957) and Ricker (1975) models, together with other formulations such as those proposed by Deriso (1980), Cushing (1973), and Shepherd (1982).

The classical approach to S-R relationship assumes the existence of a functional relationship, $F(\cdot)$, between spawning stock biomass, S_t , and recruits, R_t , over some time (usually years) of $t = 1, \dots, n$, which can be expressed as:

$$R_t = F(S_t, \Theta), \quad (2.1)$$

where Θ is a vector of parameters. Deriso (1980) introduced the general three-parameter S-R relationship, which was further developed by Schnute (1985). The resulting Deriso-Schnute model,

$$R_t = aS_t(1 - \gamma bS_t)^{1/\gamma}, \quad (2.2)$$

is such that

$$R_t = \begin{cases} aS_t e^{-bS_t}, & \lim_{\gamma \rightarrow 0} \\ \frac{aS_t}{1 + bS_t}, & \gamma = -1. \end{cases} \quad (2.3)$$

The models resulting from setting $\lim_{\gamma \rightarrow 0}$ and $\gamma = -1$ define, respectively, the Ricker (1975) and the Beverton and Holt (1957) models, which are the most commonly used, and the ones that I dealt with alongside this work.

According to Hilborn and Walters (1992), the predominant assumption was that the errors in the S-R relationship were usually lognormally distributed, and consequently, a stochastic version of the classical models, given lognormal errors, could be formulated as

$$R_t = F(S_t, \Theta)e^{\varepsilon_t}, \quad (2.4)$$

where $\varepsilon \sim N(0, \sigma^2 I)$. Abusing notation slightly, from this point onward I denoted the S-R relationship as: $R(S) = F(S, \Theta)$.

2.3.1 Beverton and Holt's model

The S-R curve proposed by Beverton and Holt (1959), presented below, has historically been highly valuable and widely used due to its straightforward interpretation and tractability. Several formulations exist, but the most well-known, and the one employed throughout this study, is the following:

$$R(S) = \frac{a \cdot S}{b + S},$$

where S represents spawning stock biomass (SSB), $R(S)$ is the recruitment expressed as a function of S , a is a parameter corresponding to the asymptotic maximum recruitment, and b is the average productivity parameter, i.e., the biomass level that produces, on average, a recruitment equal to $\frac{a}{2}$.

The Beverton-Holt curve is based on the assumption that juvenile competition results in a mortality rate that depends linearly on the number of fish alive in the cohort at any given time (Hilborn and Walters, 1992). In Figure 2.5, an example of a Beverton-Holt curve is shown, illustrating the typical behavior of this S-R relationship, where recruitment stabilizes toward an asymptote due to intraspecific competition or other factors.

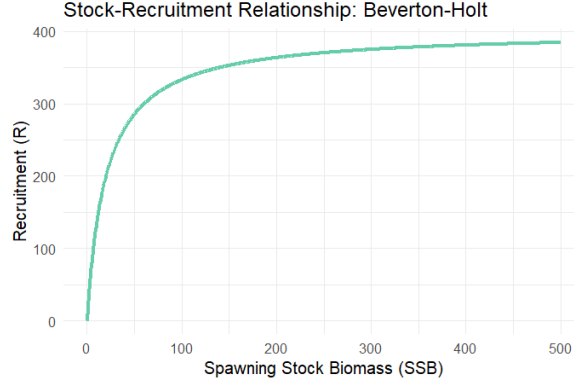


Figure 2.5: Beverton-Holt model curve.

2.3.2 Beverton-Holt's model with autoregressive component

As previously mentioned, the most common assumption is that the errors in the spawner-recruitment relationship are usually lognormally distributed (Hilborn and Walters, 1992). However, there is evidence that non-parametric and Box-Jenkins models can be used for consideration of other types of error structures other than lognormal (Meyer and Millar, 1999).

For example, I can consider a Beverton-Holt model with an ARMA structure for the error. An ARMA model, defined by Box and Jenkins (1976) is an attempt to describe a time-series in terms of combined autoregressive (AR) and moving average (MA) effects. A general ARMA(p, q) model fitted to a series x_i is formulated as:

$$x_i - \phi_1 x_{i-1} - \dots - \phi_p x_{i-p} = a_i - \theta_1 a_{i-1} - \dots - \theta_q a_{i-q},$$

where p and q are the order of the AR (autoregressive) and MA (moving average) components; and ϕ_i and θ_i are the respective parameters to be estimated, while $a_i \sim N(0, \sigma^2)$ are independent identically-distributed random variables also known as innovations.

In this case, we were dealing with the residuals of a fitted parametric model, so their mean will tend to fluctuate around 0 without the need of further intervention. Moreover, in the exploratory analysis conducted before it was inferred that the autocorrelation is of order 1 (since the significant correlation appeared at Lag 1). In conclusion, there is evidence to consider an ARMA(0, 1), or abbreviatedly $AR(1)$ model.

The baseline relationship between spawning stock biomass (S) and Recruitment (R) in year t follows the classical Beverton-Holt function:

$$R(S) = \frac{a \cdot S}{b + S} \cdot e^{\varepsilon_t},$$

where ε_t is an error term, which in standard models is assumed to be independent, but in the $AR(1)$ model follows the structure:

$$\varepsilon_t = \rho \cdot \varepsilon_{t-1} + \eta_t,$$

where ρ is the autocorrelation coefficient, ε_{t-1} is the residual from the previous year, and η_t is Gaussian white noise. While the standard model assumes that recruitment deviations are independent random noise, the $AR(1)$ model acknowledges that stock productivity has temporal memory.

2.3.3 Ricker's model

Ricker (1954) proposed an alternative to the Beverton-Holt curve, whose most common parameterization (and the one used in this study) is as follows:

$$R(S) = aS \cdot e^{-bS},$$

where $R(S)$ and S denote recruitment and SSB , respectively. Note that the parameters a and b have a different interpretation than in the Beverton-Holt model. The parameter a represents the maximum reproductive rate of the population. It acts as a scaling factor that determines the maximum value that R can reach when biomass S is low.

Similarly, the exponential term reflects a decrease in reproduction due to intraspecific competition or other density-dependent factors. In other words, b determines how rapidly reproduction declines as population biomass increases.

The biological assumption behind Ricker’s model is that the mortality rate of the eggs and juveniles is proportional to the initial cohort size, that is, mortality is stock-dependent rather than density dependent. At high biomass levels, recruitment decreases to a greater or lesser extent (Figure 2.6). Four commonly discussed mechanisms that can lead to a Ricker-shaped recruitment curve are cannibalism of the juveniles by the adults, disease transmission, damage by adults of one another’s spawning sites, and density-dependent growth coupled with size-dependent predation (Hilborn and Walters, 1992).

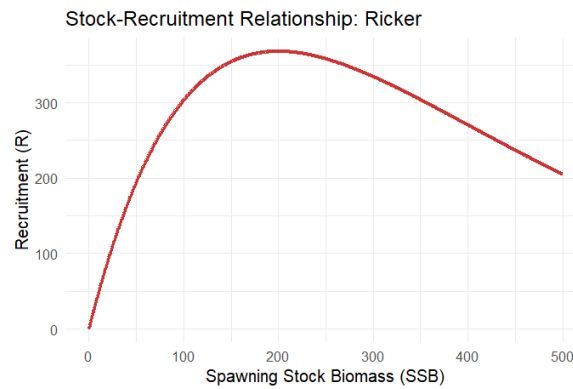


Figure 2.6: Ricker model curve.

2.3.4 Segmented regression model or Hockey-Stick

Even the simplest S-R models can have important implications for fisheries management. Classical models, such as Beverton-Holt and Ricker, assume that spawner-survival rate ($R(S)/S$) increases strictly as spawning biomass decreases, implying that very depleted populations would have a high capacity for recovery. However, this assumption may be biologically unrealistic and may lead to an overestimation of resilience and an underestimation of extinction risk. Empirical evidence, such as in the case of coho salmon (*Oncorhynchus kisutch*) presented in Barrowman and Myers (2000), suggested that survival may remain approximately constant at low densities and only decline once habitat limitations are reached, contradicting these formulations.

In this context, Barrowman and Myers (2000) proposed the use of an alternative model known as segmented regression or “Hockey-Stick”, named after the shape of its curve, in which recruitment is proportional to biomass at low abundance and stabilizes beyond a threshold. This approach avoided the assumption of unbounded increases in survival at low densities and could provide more realistic estimates for management purposes, even when the statistical fit was similar to that of traditional models.

This model is defined as follows:

$$R(S) = \begin{cases} aS, & \text{if } S \leq b \\ ab, & \text{if } S > b \end{cases}$$

where $a > 0$ is the slope at the origin (recruitment per spawner rate at low densities), and b is the breakpoint or threshold beyond which recruitment remains constant, while $R(S)$ and S are the

previously defined recruitment and spawning biomass, respectively. In the example plot shown in Figure 2.7, the shape of this function can be observed: it is linear up to a critical point b , beyond which recruitment stabilizes.

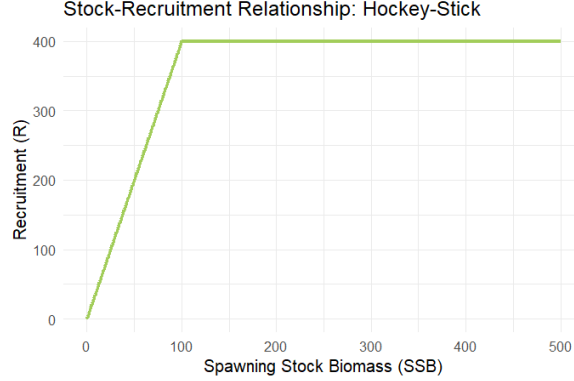


Figure 2.7: Hockey-Stick model curve.

2.4 Uncertainty estimation using residual bootstrap

After the analysis of the S-R relationship, I conducted a more detailed analysis of the uncertainty. For the analysis of the relationship between the explanatory variable (SSB) and the response variable (recruitment), I started from the general framework of a regression model defined as:

$$Y = m(X) \cdot e^\varepsilon$$

where Y represents the response variable and X the explanatory variable. In this formulation, $m(x) = E(Y | X = x)$ defines the conditional mean or regression function, while e^ε represents the random error term, assumed to follow a lognormal distribution (Haddon, 2011).

A residual bootstrap resampling procedure was implemented to quantify the uncertainty associated with the estimation of the parameters a and b . In this approach, the explanatory variables were kept fixed, and resampling was applied exclusively to the model residuals. This method captures the uncertainty around the regression function $m(x)$ while preserving the original predictor structure, which is particularly useful in time series where the stability of explanatory variables is essential for parameter estimation (Cao, 2022). In each replicate, the vector of lognormal residuals from the Beverton-Holt model was resampled with replacement. A bootstrap recruitment vector (response variable) was then simulated using the resampled residuals, and a new Beverton-Holt model was fitted using the original explanatory variable (SSB) and the bootstrap recruitment values. The parameters a and b estimated in each iteration were stored to construct their empirical distributions.

In the particular case of the Beverton-Holt autoregressive model, I computed the innovations (w_t), representing white noise once the memory induced by autocorrelation ρ had been removed. For each of the $n = 2000$ iterations, I resampled with replacement from the vector of innovations, obtaining a bootstrap innovation vector w_t^* . From this, I reconstruct the model errors (ϵ_t^*) using the original autocorrelation coefficient (ρ_0) as follows:

$$\epsilon_t^* = \rho_0 \epsilon_{t-1}^* + w_t^*.$$

Bootstrap recruitment values R_t^* are then generated as before, and the model is refitted for each simulated series.

2.5 Stochastic simulation for Biological Reference Points

Once the S-R relationship analyses have been carried out, I shifted to calculating the biological reference points (BRPs), that is, the indicators of the exploitation status and the recovery capacity of this stock. To do this, I employed the EqSim stochastic simulation framework (ICES, 2017), which provided MSY BRPs based on the equilibrium distribution of long-term projections.

By definition, a population is said to be at equilibrium when

$$\frac{dN}{dt} = 0,$$

where N denotes the number of individuals and t represents time; that is, when the rate of change in population size is equal to zero. Trivially, this condition is satisfied if the population is extinct ($N = 0$). If $N \neq 0$, the population is at equilibrium when the birth rate (i.e., the number of individuals born each year) and the mortality rate are exactly equal. The mortality rate (Z), that is, the number of individuals dying each year, can be expressed as the sum of natural mortality (denoted by M), corresponding to individuals that die from natural causes such as disease, predation, and other environmental factors, and fishing mortality F . Therefore, $Z = M + F$.

In both cases, I assumed the absence of immigration, meaning that the only changes in the number of individuals within the stock were due to births and deaths. This is a particularly relevant concept in fisheries management because, for a non-extinct population with positive birth and mortality rates, equilibrium conditions generally indicate a healthy ecological state of the population (Kilduff et al., 2009). If birth and mortality rates remain constant but a perturbation in population size occurs, possibly due to immigration or emigration, a new equilibrium population size will eventually be established. Under this state, the following condition holds:

$$N_{t+1} = N_t,$$

When populations are not at equilibrium, they will either grow without bound or decline towards extinction at a rate determined by the difference between births and deaths (Haddon, 2011).

The simulation is initialized using the outputs of the SS3 model conducted previously, which provides us the historical time-series of abundance-at-age, fishing mortality, and biological parameters. EqSim bridges the gap between past observations and future projections by resampling the parameters of natural mortality (M), weights-at-age (W_a), maturity-at-age, and selectivity (S_a) from the most recent years of the assessment. In this study the last 3 years of the assessment were used. This ensured that the simulations reflected the current productivity regime of the ecosystem (Hillary, 2009).

Unlike deterministic models that settled on a single point, EqSim evaluated the stochastic equilibrium, providing a probability density function of potential outcomes for any given fishing mortality F . The underlying biological operating model follows a discrete-time Markovian process. The abundance of the population at age a and year $y + 1$ is determined by the state of the cohort in the previous year, governed by the survival equation:

$$N_{y,a} = N_{y-1,a-1} e^{-(M_{y-1,a-1} + F \cdot S_{y-1,a-1})}$$

For the plus-group (A^+), the model accounts for the accumulation of older individuals as

$$N_{y,A^+} = N_{y-1,A^+-1} e^{-Z_{y-1,A^+-1}} + N_{y-1,A^+} e^{-Z_{y-1,A^+}},$$

where Z is defined as the total mortality rate ($Z = M + F$). This structure assumes that at equilibrium, the age structure across years becomes equivalent to the age structure within a single year. That is, the abundance of a specific age group remains stable in probability across subsequent years if the harvesting rate is constant.

Consequently, the *SSB* at equilibrium (S_{eq}) is defined as:

$$S_{eq} = SPR(F) \cdot R(S_{eq})$$

where $SPR(F)$ is the Spawning Per Recruit, the lifetime contribution of a recruit to the SSB at a given fishing mortality F . The spawner-per-recruit is defined as a function that evaluates the ratio of spawning biomass to recruits for a given level of fishing mortality:

$$SPR(f) = \sum_a Mat_a W_{a,b} e^{-\sum_{j=1}^{a-1} Z_j} \quad (2.5)$$

where Mat_a is the maturity-at-age, $W_{a,b}$ is the beginning-of-year (i.e., stock) weight-at-age, and the exponentiated term represents the cumulative sum of total mortality up to a given age, as indicated by a standard cohort equation, which yields the ratio of abundance-at-age to recruit abundance.

The Maximum Sustainable Yield (MSY) is found by identifying the global optimum of the equilibrium yield curve (Y_{eq}) with respect to F :

$$Y_{eq}(F) = YPR(F) \cdot R_{eq}(F)$$

The yield-per-recruit (YPR) is calculated using the Baranov catch equation to determine the proportion of the cohort (P_a) harvested at each age:

$$YPR(F) = \sum_a P_a W_a^m e^{-\sum_{j=1}^{a-1} Z_j}, \quad \text{with } P_a = \frac{F_a}{Z_a} (1 - e^{-Z_a})$$

In EqSim, these equations are solved numerically using optimization algorithms (e.g., `nlminb` in R). This allows for the inclusion of complex, non-linear S-R relationships such as the Beverton-Holt or the segmented regression, the latter being the standard for precautionary management (ICES, 2022).

The core strength of EqSim lies in its ability to integrate uncertainty. Recruitments were resampled from their predictive distribution based on the fitted S-R relationship, often incorporating model averaging via smooth AIC weights (Buckland et al., 1997). To account for the real-world conditions of fisheries management, EqSim incorporated assessment error and autocorrelation, using ICES default values (ICES, 2015). The simulations were typically run for 200 years, with the final 50 years retained to compute stable equilibrium values. This process yielded a probability density function for Y_{eq} , where F_{MSY} is defined as the rate that maximizes the median yield. (Gullage et al., 2017).

2.5.1 Biological Reference Points

There are two categories of BRPs used in fisheries management for this type of stock: precautionary approach (PA) reference points, which define precautionary thresholds intended to reduce the risk of stock depletion and as proxies to avoid exceeding critical stock states; and MSY reference points, which are intended to provide advice consistent with the objective of achieving MSY (ICES, 2024). The management of marine resources has evolved from an framework primarily focused on the PA during the late 1990s, aimed to prevent stock collapse through the establishment of critical biomass thresholds such as B_{lim} , toward the subsequent integration of the MSY framework following international commitments in the 2000s onward (Silvar-Viladomiu et al., 2022). This transition required the development of advanced methodologies and computational tools based on stochastic simulation, such as the aforementioned EqSim, implemented in the R `msy` package, which has become the technical standard adopted by ICES.

Table 2.1 lists the purpose and theoretical basis of each BRP estimated throughout this work. All biomass reference points are expressed in units of SSB , unless otherwise indicated.

According to the official ICES guidelines and following a PA, the final value of F_{MSY} must necessarily be constrained by precaution, implying that F_{MSY} should never exceed $F_{p05} = F_{pa}$ (Winker, 2025).

Long-term reference points were estimated based on 2001 simulations projected for 200 years over a range of F values using stochastic simulations. MSY reference points were estimated based on these simulated populations with the estimated S-R relationship segmented regression model with a fixed breakpoint at B_{lim} , along with a Beverton-Holt and Beverton-Holt AR(1) model. To reflect the

current patterns of population dynamics and exploitation, the simulations used the average selectivity and weight-at-age values from the most recent three years. Uncertainty in SSB and F was based on the estimates from the final year of the benchmark assessment, with $\sigma_{SSB} = 0.17$ and $\sigma_F = 0.14$. Assessment error was configured using the default values ($cv_F = 0.212$, $\phi_F = 0.423$), and the option `rhologRec = TRUE` was included when necessary to account for the autocorrelation present in recruitment (Table 2.2).

The SSB for our stock shows a stable and narrow dynamic range and recruitments with occasional strong year classes, and there is also no evidence of reduced reproductive capacity at any of the observed SSB levels. Following the ICES guidelines for this particular type of stock (ICES, 2021), B_{pa} was set equal as the minimum observed SSB in the available time series (1992-2024) in the benchmark assessment (ICES, 2024) to $B_{loss} = 274 kt$ (thousand tonnes). A proxy for B_{lim} was derived as $B_{lim} = B_{pa} \cdot \exp(-1.645\sigma) = 217497$ with σ as the standard deviation of SSB . When used, $MSY B_{trigger}$ was set equal to B_{pa} .

$MSY B_{trigger}$, or $B_{trigger}$, is a reference point established as a precautionary threshold for implementing management actions aimed at reducing the risk of the stock falling below critical biomass levels (B_{lim}). The Harvest Control Rule (HCR) established by ICES, which can be consulted in Azevedo et al. (2017), states that when $SSB \geq B_{trigger}$, the fishing mortality rate may be gradually increased until reaching F_{MSY} . When $B_{lim} < SSB < B_{trigger}$, fishing pressure must be reduced according to the following formula:

$$F = F_{\text{by-catch}} + \frac{F_{\text{MSY}} - F_{\text{by-catch}}}{\frac{B_{\text{trigger}} - B_{\text{lim}}}{SSB - B_{\text{lim}}}},$$

where $F_{\text{by-catch}}$ is the fishing mortality applied when $SSB \leq B_{lim}$ (Figure 2.8).

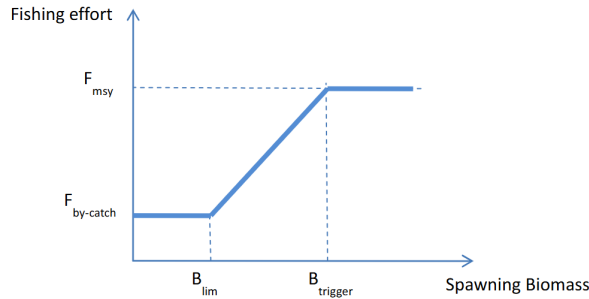


Figure 2.8: Harvest Control Rule (HCR) established by ICES.

2.5.2 Biological Reference Points: a deterministic approach

In contrast to the EqSim software, which provided reference points based on Monte Carlo simulations projecting the stock into the future until equilibrium was reached, the FLR ecosystem (which will be discussed in detail later) includes the FLBRP (FLR Reference Points) package, designed to estimate reference points based on analytical yield-per-recruit models and deterministic equilibrium calculations (Kell et al., 2007). It is based on the direct solution of analytical equilibrium equations over mean parameter vectors and allows the calculation of a wide range of classical biological reference points grouped into three main categories: reference points based exclusively on per-recruit analysis, which do not require the definition of a stock-recruitment relationship since recruitment is assumed to remain constant and independent of biomass; equilibrium-based reference points with stock-recruitment relationships (Beverton-Holt, Ricker, etc.), where long-term equilibrium points are calculated mathematically and directly (ICES, 2022); and economic reference points, such as F_{mey} (Maximum Economic Yield), defined as the fishing mortality that maximizes net economic profit by combining catch-value

curves with fishing-effort costs. In [Annex A](#), Table 2 summarizes the reference points estimated in this study using FLR.

Using the Beverton-Holt and Beverton-Holt AR(1) models in a comparative framework, I estimated the BRPs using this approach.

Table 2.1: The definition and basis of precautionary approach (PA) and MSY reference points used by ICES to assess the state of stocks and exploitation.

PA reference point	Definition	Basis
B_{lim}	A deterministic biomass limit below which a stock is considered to have reduced reproductive capacity.	The biomass below which recruitment reduces with spawning-stock biomass.
F_{lim}	Exploitation rate which leads SSB to B_{lim} .	The fishing mortality rate (F) that in stochastic equilibrium will result in median (SSB) = B_{lim} (i.e. 50% probability of SSB being above or below B_{lim}).
B_{pa}	A stock status reference point above which the stock is considered to have full reproductive capacity, having accounted for estimation uncertainty.	The value of the estimated SSB , which ensures that the true SSB has less than 5% probability of being below B_{lim} , i.e. the 95th percentile of the distribution of the estimated SSB if the true SSB equals B_{lim} .
F_{pa}	An exploitation rate reference point below which exploitation is considered to be sustainable, having accounted for estimation uncertainty.	The fishing mortality including the advice rule that, if applied as a target in the ICES MSY advice rule (AR) would lead to $SSB \geq B_{lim}$ with a 95% probability (also known as F_{p05}).
MSY reference point	Purpose	Basis
F_{MSY}	The F expected to give maximum sustainable yield in the long term.	F that provides maximum yield, given the current assessment/advice error, constrained so that the long-term probability of $SSB < B_{lim}$ is $\leq 5\%$: $F = F_{MSY}$ (if $SSB \geq MSY B_{trigger}$) $F = F_{MSY} \cdot SSB / MSY B_{trigger}$ (if $SSB < MSY B_{trigger}$).
MSY $B_{trigger}$	A lower bound of the expected range of SSB when the stock is fished at F_{MSY} .	Usually, MSY $B_{trigger} = B_{pa}$.

Table 2.2: EqSim settings used in simulation to determine reference points for horse mackerel.

Setting	Value
Number of simulations	2001
Assessment uncertainty	
σ_F	0.17
σ_{SSB}	0.14
Stock-Recruitment Relationship (S-R relationship)	
Models	Segmented regression with fixed breakpoint (SegregB _{lim}), Beverton-Holt, Beverton-Holt AR(1), and model averaging (Buckland et al., 1997)
Year range	Full time series (no years excluded)
Autocorrelation in recruitment	Used ($\rho_{Rec} = \text{TRUE}$) in BH-AR(1)
Biology (Weight-at-age)	
Year range for resampling	Last 3 years (2022-2024)
Type	Constant/Average (bioConst = TRUE)
Selectivity	
Year range for resampling	Last 3 years (2022-2024)
Type	Constant/Average (selConst = TRUE)
Advice uncertainty (Forecast error)	
cv_F	0.212 (default)
ϕ_F (autocorrelation in F error)	0.423 (default)
cv_{SSB}	0

2.6 Sensitivity analysis

I carried out a sensitivity analysis on a set of parameters (steepness, virgin recruitment and γ) for the Beverton-Holt model. I employed the standard Beverton-Holt model, as it was the most commonly used formulation in the literature on horse mackerel stock assessment. This choice allowed us to compare the estimated optimal values with those historically used in previous studies.

2.6.1 Steepness

Stock productivity is a fundamental key in fishery stock assessment, since productivity influences stock size, yield, and the calculus of BRPs. When a stock is depleted to low SSB levels, its regenerative capacity (resilience) becomes crucial to its recovery. A common measure of stock resilience is the steepness (h) of the underlying stock-recruitment relationship (Lee et al., 2012). This parameter directly relates to productivity and yield and is an important element in the calculation of many management reference points.

According to Miller and Brooks (2021), steepness is “the proportion of equilibrium unexploited recruitment (the recruitment that would occur in the absence of fishing pressure, denoted as R_0) produced by 20% of unexploited spawning stock size, denoted as SSB_0 ”. Steepness is a dimensionless parameter, and it’s used to reparametrize the stock-recruitment relationship (S-R relationship) with respect to virgin spawning biomass and recruitment, S_0 and R_0 , respectively.

In the literature, the classical equations (Beverton-Holt and Ricker) have also been reformulated to provide direct information about the productivity and resilience of a fish stock, and hence to management. The Beverton-Holt (BH) model with the Steepness-Virgin recruitment formulation is defined as:

$$R(S) = \frac{4R_0hS}{(1-h)R_0\phi_0 + (5h-1)S}$$

where h is the steepness parameter, R_0 the virgin recruitment (which will be discussed in detail in the following subsection) and $\phi_0 = \text{SPR}(0)$ is the spawners-per-recruit (SPR) at unexploited conditions.

Steepness is one of the most uncertain population dynamic quantities, and determining its value may result quite challenging (Lee et al., 2012). This is linked to the fact that there is usually a lack of estimates of recruitment at either low spawning stock size or a lack of contrast in spawning stock size. A high steepness value is indicative of a resilient population, which is robust to harvesting, including a high probability of rebuilding when fishing pressure is relaxed (Subbey et al., 2014). Steepness is independent of population size and is therefore comparable across stocks.

The procedure for determining the optimal steepness (h) was carried out using the following approach. First, virgin spawning biomass per recruit (SPR_0) was deterministically derived from the stock’s biological vectors of weight-at-age, maturity-at-age, and cumulative survival-at-age. Subsequently, an initial parametric estimation was performed under the reparameterized Beverton-Holt model (`bevholtSV`). Since the estimation of steepness often exhibits high instability due to the intrinsic noise present in stock and recruitment observations, this was implemented by scanning across a continuous spectrum of fixed h values (from 0.20 to 0.99). Finally, the selection of the optimal h value was based on the AIC, the BIC and the RMSE, thereby identifying the steepness configuration that provided the best fit to the historical time series.

In order to assess the robustness of this result, two alternative configurations were implemented in the integrated assessment model Stock Synthesis (SS3): the first fixed the parameter at the value obtained from the sensitivity analysis, whereas the second allowed the SS3 framework itself to estimate h freely.

2.6.2 Virgin recruitment

Virgin recruitment, formally denoted as R_0 , constitutes one of the most critical scaling parameters in population dynamics modelling (Quinn and Deriso, 1999). From a technical perspective, this parameter

is defined as the average number of recruits, that is, young individuals that reach the threshold age or size required to enter the exploitable fraction of the population, that a stock is capable of producing sustainably under equilibrium conditions and in the complete absence of fishing pressure (Hilborn and Walters, 1992).

The biological significance of R_0 is directly reflected in its mathematical relationship with virgin spawning biomass (S_0 or SSB_0). Virgin spawning biomass, SSB_0 , is derived from R_0 as follows:

$$SSB_0 = R_0 \cdot \phi_0$$

where ϕ_0 or SPR_0 represents the potential reproductive output that a single recruit would contribute throughout its life cycle in the absence of fishing mortality (Mace and Doonan, 1988).

In contemporary fisheries management practice, the robust estimation of R_0 is essential, given that this parameter is closely linked to population resilience through the concept of steepness (h). While steepness determines the fraction of virgin recruitment that the remaining stock is able to generate when spawning biomass has been reduced to 20% of its unfished level due to human exploitation (Brooks and Powers, 2007), R_0 establishes the upper limit, or productive ceiling, of the population in its unfished state.

The procedure used to evaluate model sensitivity to virgin recruitment (R_0) consists of a parameter profiling approach through a systematic sweep of productivity scenarios. First, an unconstrained fit was performed in order to obtain a baseline reference estimate (R_0 free). Subsequently, a vector of five values proportional to this reference was defined, spanning from 50% to 150% of the estimated value. The classical Beverton-Holt model was then sequentially forced to fit each scenario using Maximum Likelihood Estimation, fixing the virgin recruitment parameter at each iteration while allowing only the remaining parameter to be freely estimated. Finally, the optimal scenario was selected by minimizing the AIC, BIC and RMSE.

2.6.3 Density-dependent effects

In the context of population ecology, density dependence refers to the process whereby the per capita growth rate of a population changes in response to the population's density or size (Hilborn and Walters, 1992). In fisheries applications, this phenomenon is responsible for regulating fish populations, preventing them from growing indefinitely or collapsing due to minor fluctuations. I consider three types of density-dependent behaviour in a stock:

- Compensatory density dependence (or compensation): as population density increases, intraspecific competition for limited resources such as food or shelter intensifies, leading to increased juvenile mortality or reduced fecundity, as described in Beverton and Holt (1957).
- Overcompensatory density dependence (or overcompensation): classically modelled by Ricker (1954, 1975) and generalised by Shepherd (1982), this occurs when increases in population density generate strongly negative effects such as adult predation on eggs and larvae (cannibalism), or the rapid spread of disease. This leads to a sharp decline in recruitment at high stock levels and may induce marked biological instability (Quinn and Deriso, 1999).
- Inverse density dependence: commonly referred to as the Allee effect, this manifests at very low population densities, where the scarcity of individuals severely reduces reproductive success due to difficulties in finding mates or increased vulnerability to predators. This creates a risk of collapse if the stock falls below a critical biological threshold (Courchamp et al., 2008).

Shepherd (1982) proposed a parametric stock-recruitment model that can be understood as a generalisation of the classical Ricker and Beverton-Holt formulations, by introducing a shape parameter that controls the nature of density-dependent effects in the population. The model is expressed as follows:

$$R(S) = \frac{a \cdot S}{1 + \left(\frac{S}{b}\right)^\gamma},$$

where the geometry of the curve is determined by the shape parameter γ , while a and b act as initial productivity and biomass scaling parameters, respectively. Thus, when $\gamma = 1$, the model is equivalent to the Beverton-Holt formulation, exhibiting purely compensatory density dependence; conversely, when $\gamma > 1$, the function incorporates overcompensatory effects, describing Ricker-like dynamics where recruitment decreases at high biomass levels. If $\gamma < 1$, recruitment continues to increase with spawning biomass without approaching an asymptotic limit. This implies an ecosystem with very weak compensatory mechanisms, where essential resources are effectively unlimited within the observed biomass range. Mathematically, at high spawning biomass, the Shepherd model with $\gamma < 1$ approaches the exponential form described by Cushing (1973) ($R \propto S^{1-\gamma}$).

To empirically evaluate the behaviour of this parameter in our stock, I implemented a sensitivity analysis. First, I defined a discrete set of scenarios by constructing a test vector with seven fixed values of γ (ranging from 0.1 to 4.0) in order to cover dynamics from subcompensatory to strictly overcompensatory regimes. Then, for each level of γ , the stock-recruitment relationship was fitted via Maximum Likelihood Estimation, fixing the shape parameter and allowing only productivity (a) and scale (b) to be freely estimated. Finally, AIC, BIC, and the RMSE were computed for each iteration in order to identify the optimal scenario and assess model robustness.

2.7 Software used

All analyses detailed in this document were conducted in R v.4.5.3 (R Team, 2026), and the code used, as well as the data inputs and outputs, can be consulted in the [TFM GitHub Repository](#).

The *Fisheries Library in R* (FLR) ecosystem FLR were used to develop the analysis. This is a collection of tools for fisheries science developed in R, designed for building simulations of fisheries models. Originally developed by ICES, FLR is an open and collaborative software framework, which provides a class and method structure in the R language specifically designed for stock modeling and assessment (Hillary, 2009). It is based on an object-oriented architecture (S4), whose fundamental component is the *FLQuant* object, a six-dimensional array that allows information to be organized across dimensions such as age or size structure, years, unit, spatial area, and iteration (Kell et al., 2007).

The data for our stock are stored in an object of class *FLStock*. This object class provides a comprehensive representation of a fish stock by integrating multiple *FLQuant* objects that describe the main system variables: biomass, recruitment, fishing mortality, natural mortality, and others. In essence, it constitutes a structured representation of population dynamics.

FLR consists of a collection of specialized libraries that interact with one another. Among the most relevant and widely used throughout this work are *FLCore*, which defines the base classes and data manipulation methods; *FLSR*, which focuses on modeling the stock-recruitment relationship; *FLBRP*, used for calculating reference points through deterministic equilibrium analysis; and *ggplotFL*, an extension that integrates *ggplot2* graphics within the FLR framework.

Chapter 3

Results

3.1 Exploratory analysis

The *SSB* and recruitment trends (Figures 2.2 and 2.3) revealed a recovery trend in the stock and an increase in the number of individuals. The recruitment time series showed high variability, with pronounced peaks in 1996-1997 and another in 2022. Between 2001 and 2010, recruitment levels were generally low. During these years, biomass also declined sharply, possibly linked to the low recruitment. From 2011 onward, the stock began to recover, as both the number of recruits and *SSB* followed an overall increasing trend.

The SLR model (Figure 3.1) was fit considering recruitment as the response variable and spawning biomass as the explanatory variable. The estimated slope was 6.127, with an associated p-value of 0.0688. The intercept had no practical interpretation in this context, as it does not make sense to consider a situation in which biomass is zero.

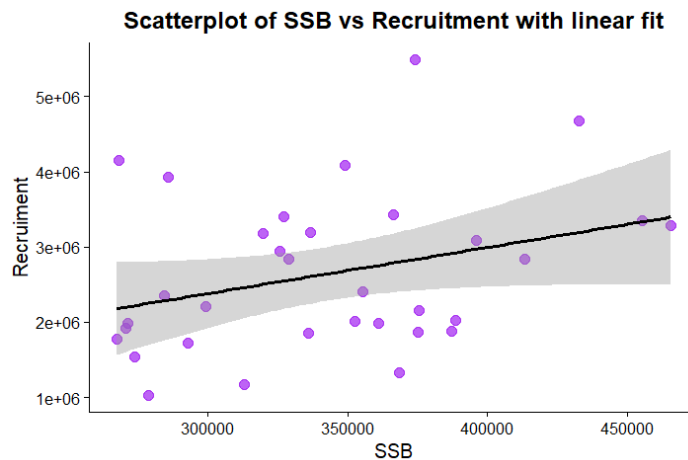


Figure 3.1: Scatter plot of *SSB* vs. recruitment with linear fit for the horse mackerel in ICES Division 9a.

The plot showed a weak positive relationship between *SSB* and recruitment. The data exhibited high dispersion, suggesting that recruitment was not driven solely by spawning biomass but was also influenced by other factors, such as environmental conditions. Although the linear model suggested a positive relationship between *SSB* and recruitment, the estimated slope was not statistically significant (p-value > 0.05).

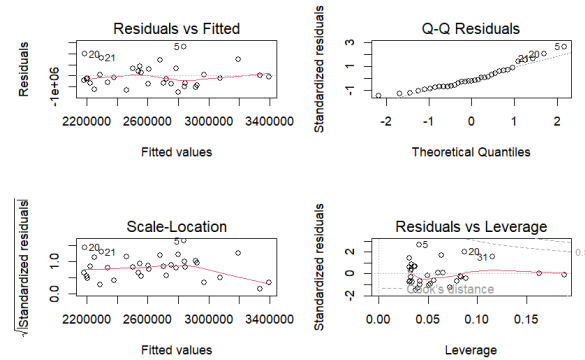


Figure 3.2: Diagnostic plots for the fitted linear regression model. (I) Residuals vs Fitted values. (II) Normal Q-Q plot of residuals. (III) Scale-Location plot. (IV) Residuals vs Leverage plot.

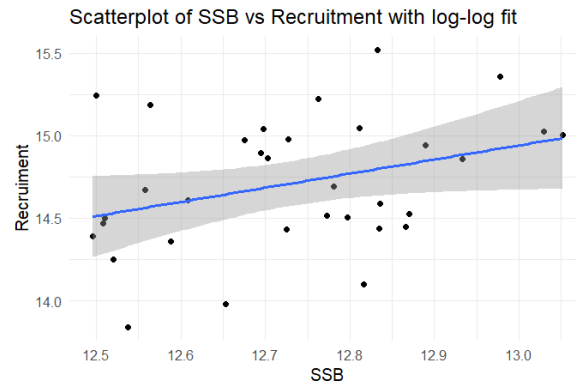


Figure 3.3: Plot of SSB vs. recruitment with log-log fit for the horse mackerel in ICES Division 9a.

The shaded confidence band was relatively wide, indicating substantial uncertainty, particularly at the extremes where fewer data points were available. SSB explained only 10% of the variability ($R^2 = 0.10$), suggesting that external factors or alternative models (such as the previously mentioned Ricker or Beverton-Holt models) may describe better the species' dynamics.

The diagnostic plots of the simple linear regression (Figure 3.2) model showed deviations from normality in the residuals and signs of heteroscedasticity. In addition, points 5, 20, and 21 (corresponding to years 1996, 2022 and 2023, respectively) appeared as outliers, with point 5 being nearly influential. This suggested the need for logarithmic transformations or the use of more flexible models such as GAMs.

Applying a logarithmic transformation slightly improved the model fit, revealing a positive relationship between the explanatory variable and the response, with an estimated slope of 0.86 (Figure 3.3). Although the p-value ($= 0.052$) for the slope estimate lied slightly above the conventional significance threshold of 0.05, the results suggested a biologically meaningful influence of SSB on recruitment, with more balanced residuals.

Next, a GAM with a smoothing spline was fitted (Figure 3.4); however, it did not provide a significant improvement over the previous models. The effective degrees of freedom (EDF) equal 1, indicating that the fitted relationship was essentially linear.

The smooth component plot revealed a positive linear relationship between SSB and recruitment, with no need for complex nonlinear terms. Residual analysis (Figure 3.5) showed acceptable behavior: the QQ-plot indicated normality, while the random dispersion of residuals against the linear predic-

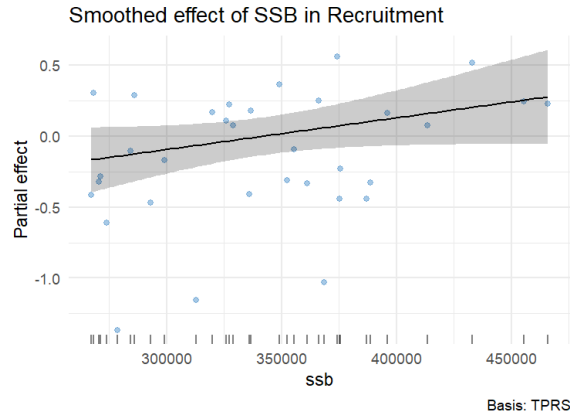


Figure 3.4: Partial smooth effect of $s(SSB)$ on the logarithm of recruitment. The central curve illustrates the spline estimated by the GAM, the shaded band represents the 95% confidence interval, and the points distributed along the curve represent the partial residuals of the model.

tor confirmed the absence of heteroscedasticity. The p-value (0.085) and the explained variability (10%) suggested that, although a positive trend exists, SSB was not the dominant factor in annual recruitment, reinforcing the idea that external environmental factors could play an important role.

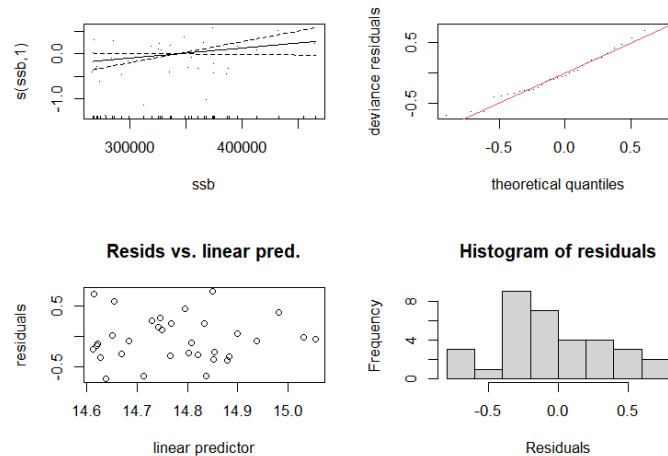


Figure 3.5: Diagnostic plots for the fitted generalized additive model (GAM). (I) Smooth term plot for the predictor SSB , showing the estimated non-linear effect together with confidence bands and partial residuals. (II) Q-Q plot of deviance residuals. (III) Residuals versus linear predictor. (IV) Histogram of residuals.

The pairs plot (Figure 3.6) showed that the marginal distributions of each variable are combined with their joint relationship. The density plots of each variable are shown along the diagonal. SSB exhibited a slightly bimodal or flattened distribution, with a strong concentration of values between 300,000 and 370,000 tonnes, followed by a pronounced decline toward higher values. This suggested that the stock has predominantly operated within intermediate biomass ranges. Examination of the marginal densities indicates that recruitment displays a marked positive skewness, characterized by a

predominance of moderate recruitment years and occasional years with exceptionally high recruitment.

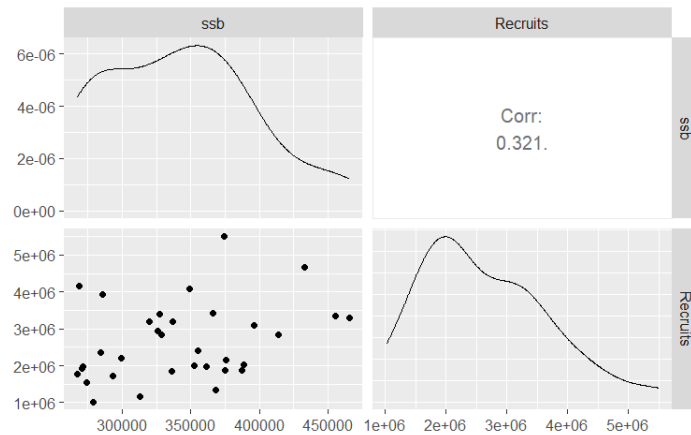


Figure 3.6: Pairs plot of the distribution of SSB and recruitment for the horse mackerel in years 1992-2024 in ICES Division 9a.

The scatter plot in the lower-left corner visually confirmed the high dispersion of the data, with no clear pattern observed. This was consistent with the GAM yielding an $EDF = 1$ (i.e., a linear relationship). Therefore, there was no evidence of density-dependent processes or significant nonlinearities within the observed biomass range. The correlation coefficient shown in the upper-right corner was 0.321, indicating a weak positive correlation. This was consistent with the R^2 values of the models (approximately 0.10), since the coefficient of determination corresponds to the square of the correlation coefficient. This result aligned with the ecology of pelagic species such as horse mackerel, where population dynamics are strongly influenced by environmental variables (ICES, 2025).

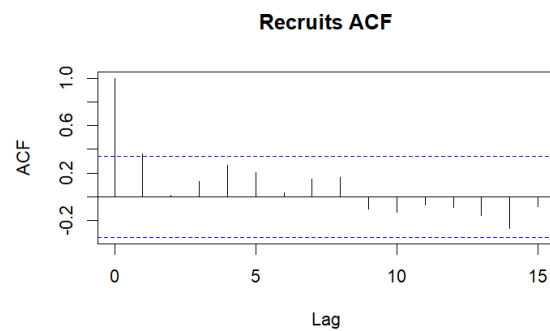


Figure 3.7: Autocorrelation function of recruitment for the horse mackerel in years 1992-2024 in ICES Division 9a.

The analysis of the autocorrelation function (ACF), (Figure 3.7) for the recruitment time series, showed a slightly statistically significant coefficients at lag = 1. This autocorrelation indicated that recruitment events were not independent across successive years.

3.2 Comparative evaluation of stock-recruitment models

3.2.1 Beverton-Holt model

Fitting the Beverton-Holt model to the 1992-2024 time series yielded productivity ($a = 2.34 \cdot 10^7$) and half-saturation ($b = 2.92 \cdot 10^6$) parameters that were significantly higher than the historically observed ranges of recruitment and *SSB*. The magnitude of parameter b relative to the maximum recorded *SSB* (approximately 465,000 t) indicated that the stock was currently in the initial ascending phase of the curve, where the relationship was effectively linear. This suggests that density-dependent effects, if present, were not yet apparent within the observed range of biomass values. Examination of the scatter plots showed that during the years 2005-2010 both recruitment and biomass declined sharply, while the most recent years (2022-2024) corresponded to the highest biomass values recorded in the time series (Figure 3.8).

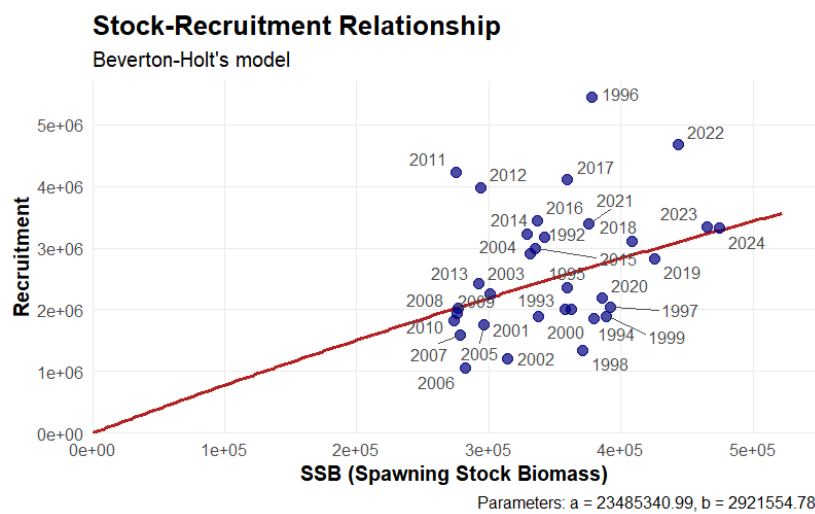


Figure 3.8: Beverton-Holt S-R model fit for Southern horse mackerel in ICES 9a and showing the slope at the origin.

Model diagnostics for the Beverton-Holt fit are presented in Figure 3.9. In the upper-left panel, the observed data are presented along with a smoothed trend (blue line). The fitted curve (red line) lied in the lower region of the data cloud, suggesting that the model may slightly underestimate recruitment at intermediate *SSB* levels, although it captured the overall increasing trend. The upper-right panel shows residuals by year, which exhibited an increasing trend, indicating the presence of positive residuals particularly in recent years. From a biological perspective, this suggested that stock productivity may have increased relative to earlier periods.

The residual autocorrelation plot (center-left panel) indicated positive correlation among residuals of successive years. That is, if the residual in one year was high, it was likely to be high in the following year as well. Such temporal dependence is common in fisheries data, as stock productivity is often influenced by periodic environmental cycles. This aspect will be explored further by incorporating a first-order autoregressive component into the Beverton-Holt model. The plots of residuals versus the explanatory variable and residuals versus the response variable showed that residuals were randomly distributed around zero, indicating homoscedasticity and linearity.

The Q-Q plot showed that residuals are approximately normally distributed, with only minor deviations from the theoretical normal quantiles. Furthermore, this model fit yielded an AIC of -44.72481 and a BIC of -41.73179 .

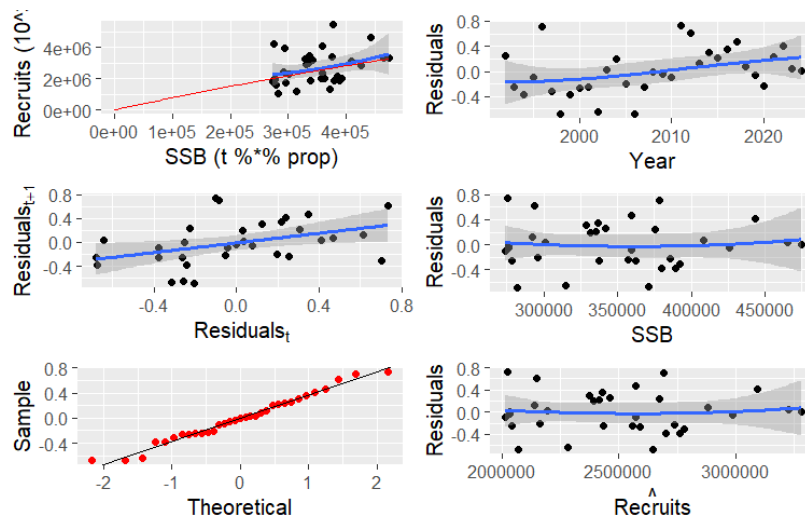


Figure 3.9: Stock-recruit FLR summary plot for Beverton-Holt model. (I) Fitted and observed relationship; (II) residuals-by-year; (III) autocorrelation trend (slope of line) in the residuals; (IV) residuals-by- SSB ; (V) qq-plot of residuals and confidence intervals; (VI) residuals-by-predicted recruitment.

3.2.2 Ricker model

Fitting the Ricker model yielded an estimate of the parameter $a = 7.96$, indicating that at low biomass levels, where the effects of density-dependent levels are negligible, each unit of SSB produces approximately 8 recruits. The density-dependence parameter ($b = 2.96 \cdot 10^{-7}$) is very small, but it has an interesting interpretation, as its inverse ($1/b \simeq 3.37 \cdot 10^6 t$) represents the biomass level at which the maximum number of recruits is achieved. Since the maximum observed SSB is around 470,000 tonnes, this implied that the stock was still in the ascending phase of the curve, and the population had the potential to grow further before intraspecific competition or cannibalism become limiting factors (Figure 3.10).

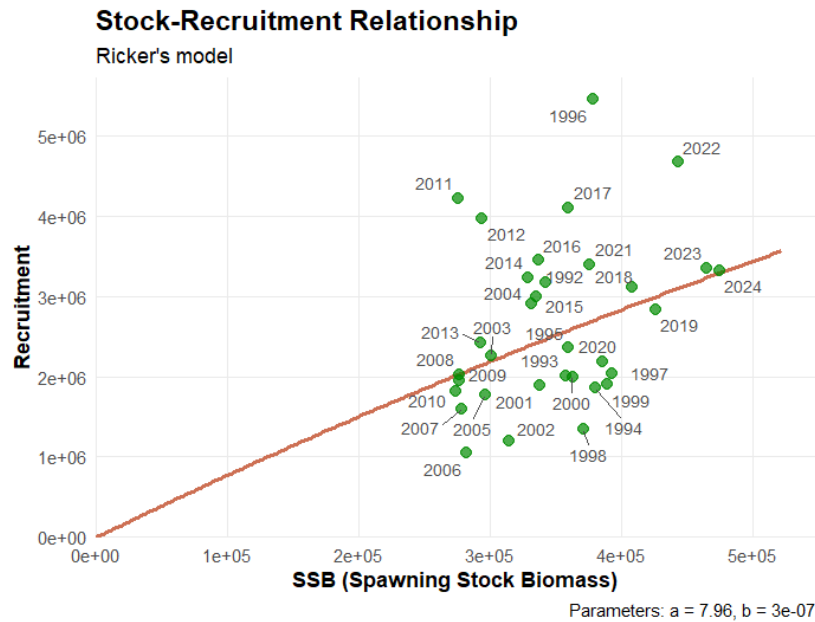


Figure 3.10: Ricker S-R model fit for Southern horse mackerel in ICES 9a and showing the slope at the origin.

The diagnostic analysis of the Ricker model showed residual behavior similar to that of the Beverton-Holt model, highlighting normally distributed errors in the Q-Q plot and constant variance. Nevertheless, the presence of a positive trend in the temporal residuals together with a marked first-order autocorrelation suggested the influence of external environmental drivers not included in the model (Figure 3.11).

According to the statistical criteria AIC and BIC, this model provided a slightly poorer fit to the Beverton-Holt model, with AIC equal to -44.7248 and BIC equal to -41.7297 . Although the differences between the two models were very small, the Beverton-Holt model was selected following the criteria proposed by Hilborn and Walters (1992), as the stock showed no biological evidence of overcompensation that would justify the use of the Ricker model at the observed biomass levels.

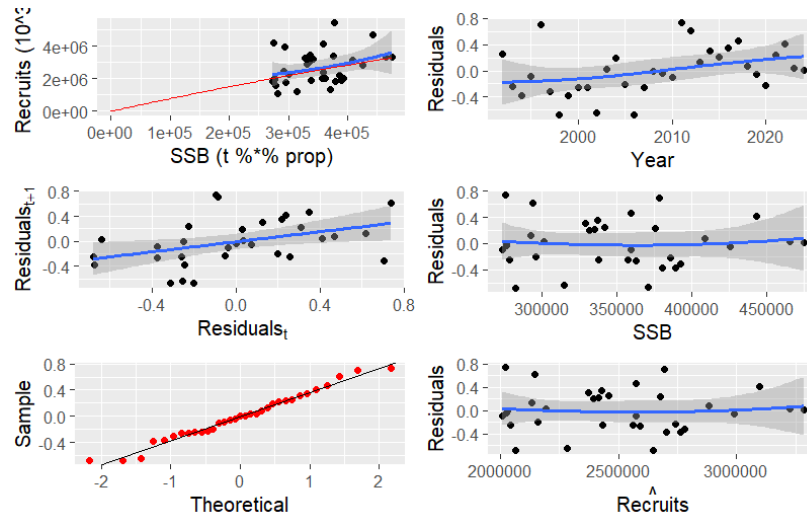


Figure 3.11: Stock-recruit FLR summary plot for Ricker model. (I) Fitted and observed relationship; (II) residuals-by-year; (III) autocorrelation trend (slope of line) in the residuals; (IV) residuals-by- SSB ; (V) qq-plot of residuals and confidence intervals; (VI) residuals-by-predicted recruitment.

3.2.3 Hockey-Stick model

The segmented regression (Hockey-Stick) model yielded an estimate of the parameter $a = 7.57$, indicating that at low levels of SSB , each additional tonne of SSB increased recruitment by approximately 7.57 thousand individuals. The estimated biological breakpoint b is 354,000 tonnes of SSB , beyond which recruitment stabilized at a plateau of approximately $a \cdot b = 2.67 \cdot 10^6$ individuals. Given that the current SSB lied significantly above this breakpoint, it could be concluded that the population is in a zone of productive stability, minimizing the risk of a decline in recruitment due to limitations in parental biomass (Figure 3.12).

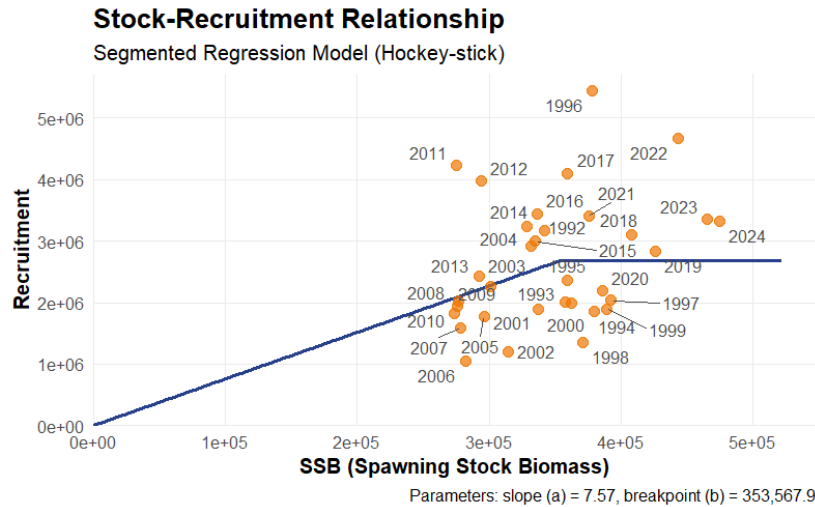


Figure 3.12: Hockey-Stick S-R model fit for Southern horse mackerel in ICES 9a and showing the slope at the origin.

The diagnostic plots (Figure 3.13) indicated that residuals were strongly negative at the beginning of the time series and become progressively more positive toward the last decade (upper-right panel). This may suggest a period of increased stock productivity, relative to early periods. In addition, the plot of residuals at time t versus $t - 1$ showed marked positive autocorrelation, reinforcing the idea that recruitment was influenced by periodic environmental cycles. The Q-Q plot indicated normally distributed errors, and the model fit yielded an AIC of -43.3178 and a BIC of -40.3248 .

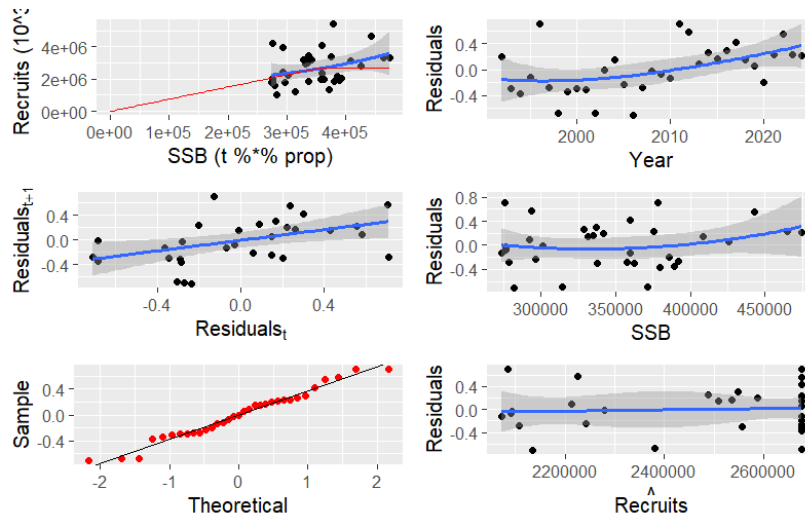


Figure 3.13: Stock-recruit FLR summary plot for Hockey-Stick model. (I) Fitted and observed relationship; (II) residuals-by-year; (III) autocorrelation trend (slope of line) in the residuals; (IV) residuals-by-SSB; (V) qq-plot of residuals and confidence intervals; (VI) residuals-by-predicted recruitment.

3.2.4 Beverton-Holt model with an autoregressive component

After evaluating the three classical stock-recruitment models, the AIC and BIC information criteria indicated a comparable support for the Beverton-Holt and Ricker formulations, whereas the segmented regression provided a slightly poorer performance. However, residual diagnostics consistently revealed the presence of marked first-order autocorrelation and temporal trends, suggesting that stock productivity is influenced by stochastic processes or environmental variability not captured by parental biomass (ICES, 2019). Therefore, I selected the Beverton-Holt model as the structural basis, given its biological stability for this species, and incorporated a first-order autoregressive component, $AR(1)$. This modification was aimed to formalize the temporal dependence observed in the residuals, allowing for more robust parameter estimation and a substantial improvement in the model's explanatory power.

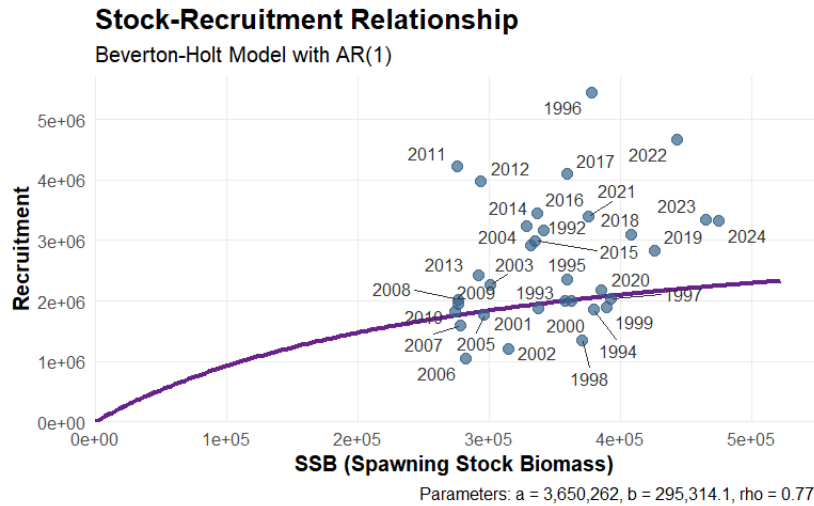


Figure 3.14: Beverton-Holt $AR(1)$ S-R model fit for Southern horse mackerel in ICES 9a and showing the slope at the origin.

This model provides an estimate of the recruitment asymptote $a = 3.65 \cdot 10^6$ and the half-saturation parameter $b = 2.85 \cdot 10^5$. The inclusion of the autocorrelation coefficient $\rho = 0.77$ meant a strong year-to-year correlation (Figure 3.14).

In the standard Beverton-Holt model (represented by the red curve in Figure 3.15), the estimator of parameter a was negatively biased by years of low productivity, particularly during the 2000s. By incorporating the first-order autoregressive component, the parameter a decreased significantly to $3.65 \cdot 10^6$, as the model identified that these observations were not independent fluctuations but belonged to periods of high and low stock productivity. The parameter b also decreased in the $AR(1)$ model, which visually translated into a curve with a gentler initial slope and a slower approach to the plateau. The reduction in Beverton-Holt parameter estimates after incorporating $AR(1)$ residual structure suggested that part of the temporal persistence previously attributed to the S-R relationship was actually due to autocorrelated process errors.

In the standard formulation, residuals were assumed to be independent and identically distributed (IID). Under this assumption, the fitting algorithm minimized the sum of squared distances (Euclidean distance) between each point and the curve. When persistent periods of unusually high or low recruitment occur, the model may adjust the biological parameters (a and b) to accommodate these observations, potentially attributing temporal changes in productivity to the S-R relationship. By incorporating the coefficient ρ , the model recognized that the error at time t was not independent but inherited part of the deviation from $t - 1$.

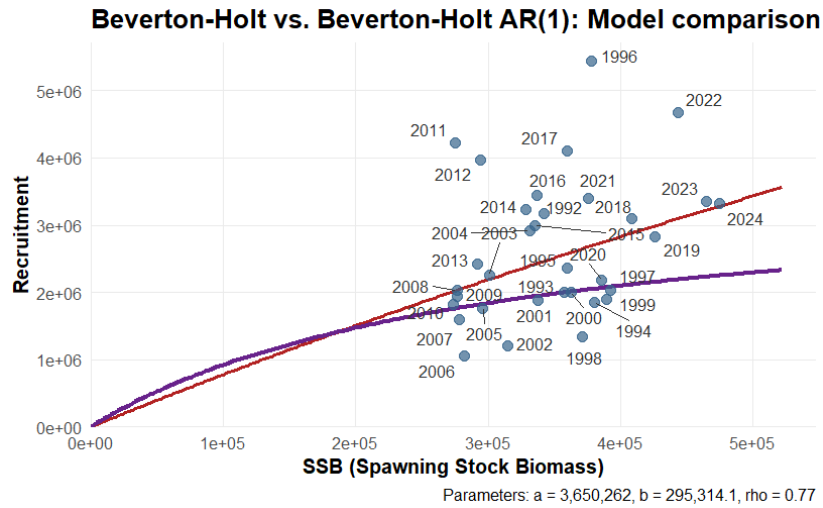


Figure 3.15: Model comparison between Beverton-Holt (red) and Beverton-Holt AR(1) S-R model (purple) fit for Southern horse mackerel in ICES 9a.

The diagnostic analysis of the Beverton-Holt $AR(1)$ model confirmed the validity of these inferences (Figure 3.16). The removal of the trend in the residuals versus time plot and, crucially, the absence of correlation in the $Residuals_t$ vs. $Residuals_{t-1}$ plot demonstrated that the autoregressive component has effectively corrected the temporal dependence in the data. Furthermore, we could see the fulfillment of normality (Q-Q plot) and homoscedasticity assumptions. These diagnostics indicated that the Beverton-Holt $AR(1)$ model provided a statistically robust description of the S-R relationship.

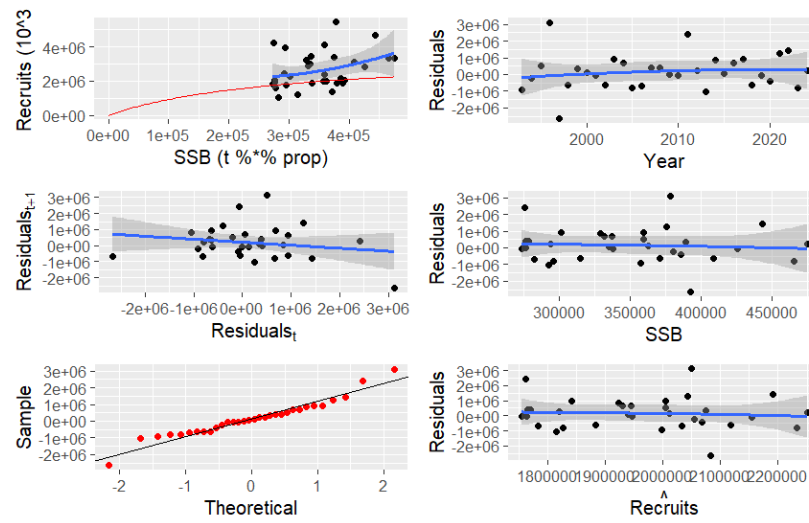


Figure 3.16: Stock-recruit FLR summary plot for Beverton-Holt AR(1) model. (I) Fitted and observed relationship; (II) residuals-by-year; (III) autocorrelation trend (slope of line) in the residuals; (IV) residuals-by-SSB; (V) qq-plot of residuals and confidence intervals; (VI) residuals-by-predicted recruitment.

3.2.5 Model comparison using AIC and BIC

Table 3.1: Estimated parameters for the fitted SR models for the horse mackerel in ICES 9a, from 1992-2024.

Model	Parameters
Beverton-Holt	$a = 2.34 \cdot 10^7$, $b = 2.92 \cdot 10^6$
Ricker	$a = 7.96$, $b = 2.96 \cdot 10^{-7}$
Hockey-Stick	$a = 7.57$, $b = 354\,000$
Beverton-Holt AR(1)	$a = 3.65 \cdot 10^6$, $b = 2.85 \cdot 10^5$, $\rho = 0.77$

Table 3.1 shows the estimated parameters for each S-R model tested. The comparison of model predictive performance was carried out using the AIC and the BIC, as shown in Table 3.2.

Table 3.2: Comparison of information criteria (AIC and BIC) for the evaluated stock-recruitment models.

Model	AIC	BIC
Beverton-Holt	-44.7248	-41.7318
Ricker	-44.7228	-41.7297
Hockey Stick	-43.3178	-40.3248
Beverton-Holt AR(1)	-47.3691	-42.8796

Among the candidate models, the Beverton-Holt model with an autoregressive $AR(1)$ structure provided the best fit, yielding the lowest values for both criteria (AIC = -47.3691; BIC = -42.8796). This model outperformed the standard Beverton-Holt and Ricker models. In contrast, the Hockey-Stick model showed notably poorer performance. The evaluation based on these criteria supported the Beverton-Holt $AR(1)$ as the most parsimonious model for describing the S-R relationship, accounting for both the biological dynamic of the stock and its temporal autocorrelation without incurring overfitting.

Figure 3.17 presents a joint comparison of the fitted models discussed in this section. For SSB levels below $2.5 \cdot 10^5$ tonnes, all models showed very similar behavior, with differences emerging at higher biomass levels. On the one hand, the Beverton-Holt and Ricker curves were almost superimposed, making them visually indistinguishable. Both suggested that recruitment continues to increase slightly or stabilizes very gradually. The segmented regression or Hockey-Stick model exhibited a pronounced “elbow” as it forced an abrupt stabilization of recruitment. Its higher AIC value suggested that the stock dynamics were not as rigid as this model assumed.

Finally, the Beverton-Holt $AR(1)$ model provided a more conservative and robust curve, as it is not affected by the bias introduced by the high recruitment peaks observed in recent years. As a result, the curve lies below the other fitted relationships at high SSB levels, providing a more precautionary perspective of the recruitment potential and, consequently, a more conservative basis for fisheries management advice.

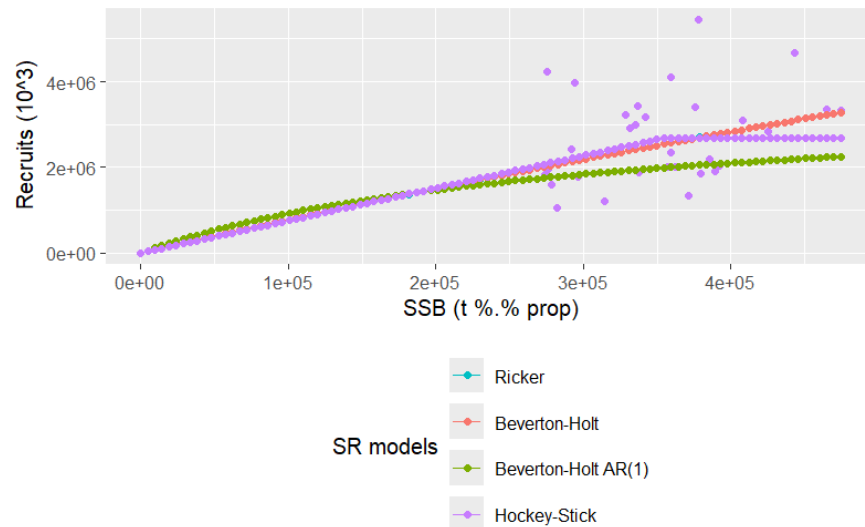


Figure 3.17: Comparison of stock-recruitment models for the horse mackerel in ICES Division 9a: Ricker (cyan), Beverton-Holt (red), Hockey-Stick (purple), and Beverton-Holt AR(1) (green).

3.3 Uncertainty estimation using residual bootstrap

The uncertainty associated with both the standard Beverton-Holt model and the Beverton-Holt $AR(1)$ model was evaluated using bootstrap resampling. The decision not to discard the standard B-H model is justified by the fact that, historically, most biological reference points used by ICES are derived from this standard stock-recruitment model due to its simplicity and the smaller number of parameters to estimate. Moreover, evaluating both models allowed us to compare the effect of accounting for temporal autocorrelation on parameter uncertainty and estimation precision.

Figure 3.18 shows the histograms of the empirical distributions of parameters a and b obtained via residual bootstrap with $n = 2000$ replicates.

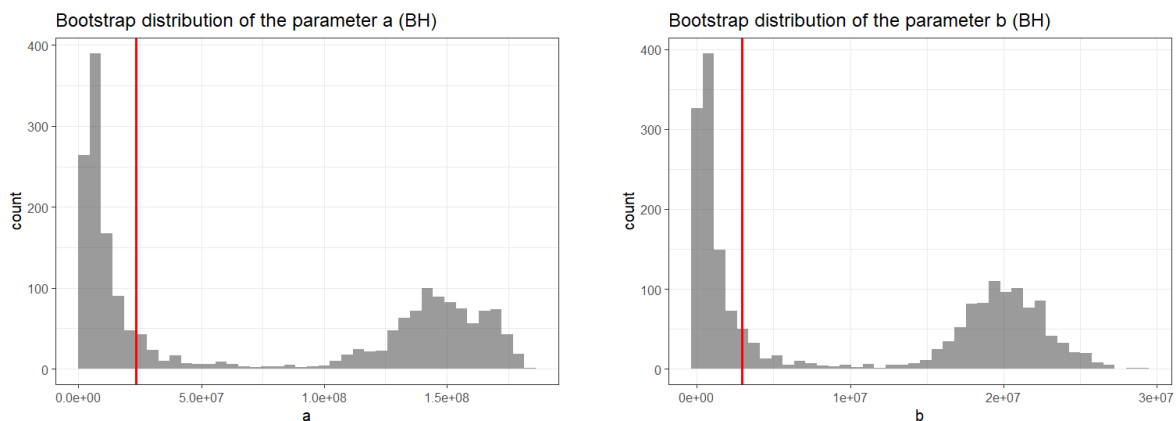


Figure 3.18: Bootstrap distributions of the parameters of the standard Beverton-Holt model ($n = 2000$). (Left) Bootstrap distribution parameter a (productivity). (Right) Bootstrap distribution of parameter b (saturation) for the B-H model.

A notable feature of the histograms is that both parameters (a and b) exhibited bimodal distributions. Table 3.3 presents the confidence intervals obtained via residual bootstrap. The bootstrap median ($2.77 \cdot 10^7$) exceeded the original estimate ($2.35 \cdot 10^7$), indicating a positive bias, i.e., the model tended to overestimate potential productivity when the data are highly dispersed. The resulting confidence intervals were extremely wide, with bounds exceeding the original estimate by nearly an order of magnitude, reflecting the instability of the standard model under high data variability.

Table 3.3: Residual bootstrap confidence intervals ($n = 2000$) for the Beverton-Holt model parameters.

Parameter	Estimate	Bootstrap Median	CI 2.5%	CI 97.5%
a (Productivity)	$2.35 \cdot 10^7$	$2.77 \cdot 10^7$	$2.77 \cdot 10^6$	$1.73 \cdot 10^8$
b (Saturation)	$2.92 \cdot 10^6$	$3.54 \cdot 10^6$	$4.79 \cdot 10^4$	$2.44 \cdot 10^7$

Having analyzed the standard model, which assumed that recruitment deviations were independent random events, the analysis was extended by incorporating the dynamic nature of marine ecosystems. I therefore implemented a residual bootstrap adapted to a first-order autoregressive process ($AR(1)$) for the Beverton-Holt model. Unlike the previous case, this approach preserved the autocorrelation structure of the error term.

The bootstrap medians for parameters a and b showed almost perfect agreement with the original estimates, indicating little or no evidence of systematic bias; this result suggested that the Beverton-Holt $AR(1)$ model provided more reliable parameter estimates despite the high variability observed in recruitment.

Table 3.4: Residual bootstrap results for the Beverton-Holt model with $AR(1)$ structure.

Parameter	Original	Bootstrap Median	CI 2.5%	CI 97.5%
a (Productivity)	$3.65 \cdot 10^6$	$3.65 \cdot 10^6$	$2.95 \cdot 10^6$	$4.34 \cdot 10^6$
b (Saturation)	$2.95 \cdot 10^5$	$2.93 \cdot 10^5$	$2.40 \cdot 10^5$	$3.52 \cdot 10^5$
ρ (Autocorrelation)	0.770	0.773	0.624	0.917

In contrast to the standard model without $AR(1)$, which exhibited bimodal parameter distributions, the distributions obtained after incorporating the $AR(1)$ are clearly unimodal, as shown in Figure 3.19, where the red line represents the original parameter estimate.

The histogram of a showed a higher density around the center of the distribution, suggesting a precise estimate of maximum productivity. In contrast, the histogram of b exhibited greater dispersion, reflecting greater uncertainty associated to this parameter, as it depended on the presence of years with very high SSB values to properly define the inflection point of the curve or carrying capacity. The histogram of the parameter ρ showed a distribution centered around 0.77, with a 95% confidence interval ranging from 0.62 to 0.91. Since the lower bound was significantly greater than zero, this confirmed that environmental or biological memory in recruitment is a dominant process. Consequently, ignoring this autocorrelation would lead to an underestimation of biomass uncertainty and an overestimation of the independence of annual recruitment events.

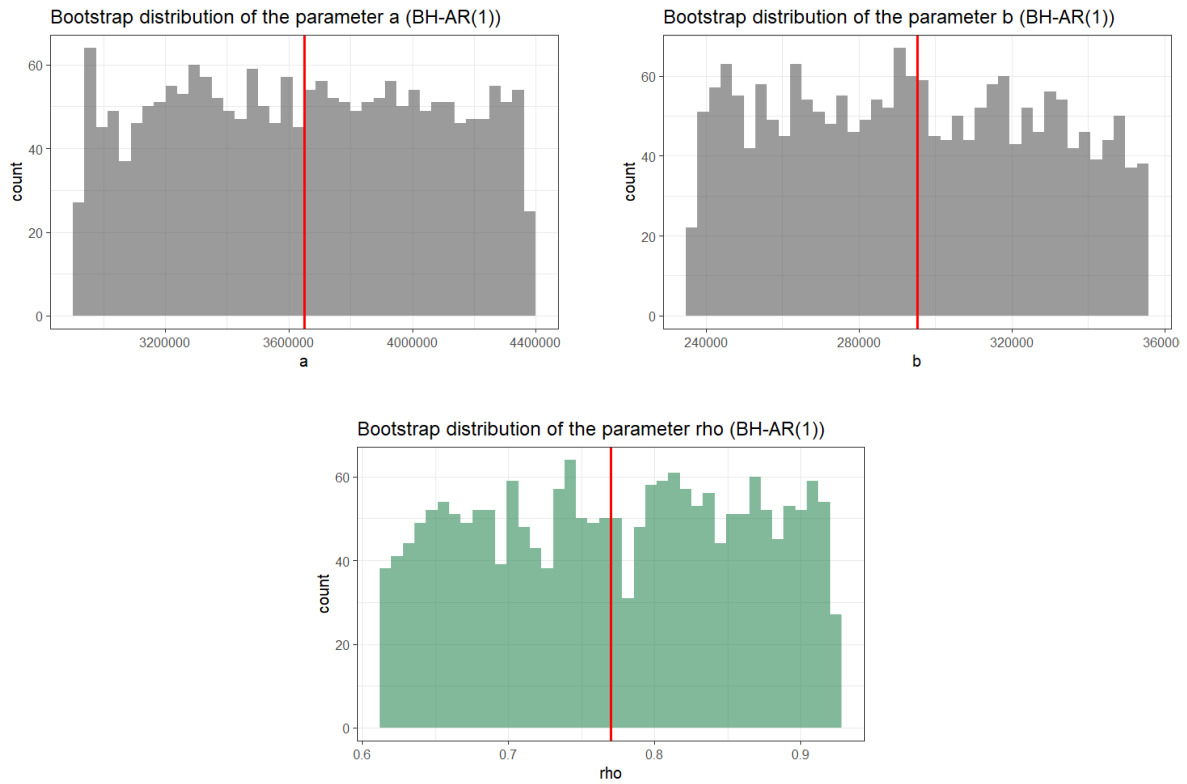


Figure 3.19: Bootstrap distributions of the parameters of the Beverton-Holt $AR(1)$ model. (Upper, left) Distribution of parameter a . (Upper, right) Distribution of parameter b . (Below) Distribution of parameter ρ .

3.4 Analysis of the S-R relationship under different productivity regimes

From the plots presented at the beginning of this chapter, I observed that the models exhibited a loss of predictive capacity after 2010 due to higher recruitment levels compared to previous years. It is therefore reasonable to explore what would happen if both periods were analyzed separately in order to assess whether significant differences exist between these two productivity regimes. Productivity regimes refer to distinct periods during which a fish stock exhibits consistent biological productivity such as recruitment driven by environmental shifts. A preliminary analysis of both time series confirmed this difference.

The boxplots of recruitment for both periods showed a substantial difference in the median values. On the one hand, the median recruitment for the years 1992-2010 was around $2 \cdot 10^6$ thousand individuals, with an isolated outlier corresponding to the year 1996. In contrast, observations after 2010 were mostly concentrated around a median of approximately $3.5 \cdot 10^6$. This observation justified the need to parameterize the S-R relationship separately in order to capture the specific dynamics associated with each productivity regime.

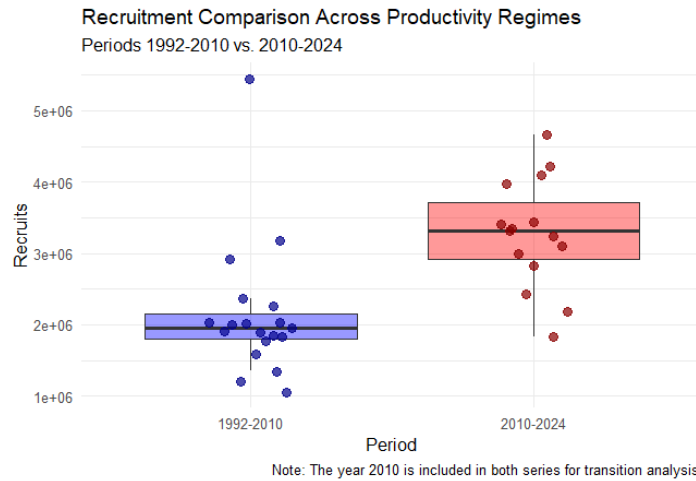


Figure 3.20: Boxplot of recruitment for the horse mackerel in ICES 9a across years 1992-2024, separated in two different time series (1992-2010 and 2010-2024).

The Wilcoxon-Mann-Whitney test yielded a p-value of 0.0001446, which is below conventional significance levels. Therefore, the null hypothesis was rejected and concluded that recruitment levels were higher from 2010 onwards. This supported the hypothesis of a positive shift in the distribution of the recruitment time series.

To further investigate these differences, I splitted the time series into two periods, establishing the breakpoint at 2010. This year was included in both series to ensure convergence of the optimization algorithm implemented in R for fitting the S-R curves. In Figure 3.21, the differences between both periods are displayed. During the years 1992-2010 (blue), recruitment was generally low, except for a peak in 1996. In 2010, the *SSB* reached its historical minimum (Figure 3.22). However, from that year onwards, both the frequency and magnitude of high recruitment events systematically increased. This increase suggested that the horse mackerel stock has entered a phase of higher productivity, possibly driven by changes in environmental conditions.

For the two separated time series, I fitted the same models as for the full series and compared their performance using AIC and BIC criteria. The selected model in this case was the segmented regression model for both periods. For the 1992-2010 period, the biological breakpoint b was estimated at $3.48 \cdot 10^5 t$, a value highly consistent with the threshold estimated for the full series ($3.54 \cdot 10^5 t$),

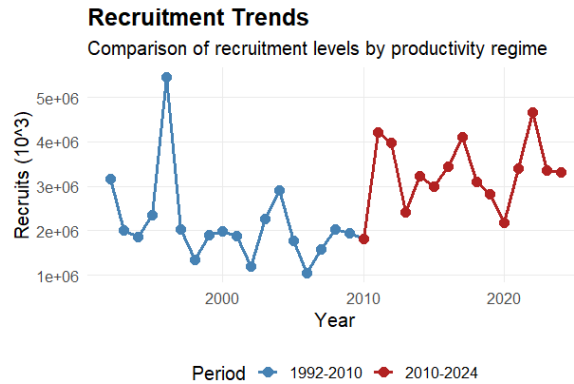


Figure 3.21: Recruitment time series for the horse mackerel in ICES Division 9a, separating the first period (1992- 2010, in blue) and the second (2010- 2024, in red).

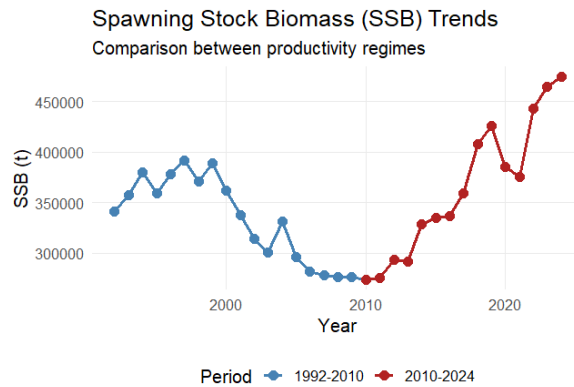


Figure 3.22: *SSB* time series, separating the first period (blue) and the second (red).

suggesting that the stock's saturation biomass has remained relatively stable over time (Figure 3.23, left). However, the initial slope estimate $a = 6.25$ was lower than that of the global model. This reduction in slope confirms the results of the Wilcoxon test, indicating that the recruitment rate per unit of spawning biomass was significantly lower during this first period before experiencing a marked increase in the last decade. This model yielded $AIC = -27.214$ and $BIC = -25.326$. Diagnostic analyses revealed a dynamic characterized by discrete recruitment levels, with a production plateau around $2 \cdot 10^6$ recruits. Despite the presence of an exceptional recruitment event in 1996, the series remained largely stable below a relatively low saturation threshold. Residual analysis suggested slight temporal autocorrelation, supporting the implementation of an $AR(1)$ error structure to capture the persistence of negative environmental anomalies affecting recruitment during this phase of low biological efficiency (Figure 3.23, right).

For the 2010-2024 period, the slope parameter of the model showed a notable increase ($a = 10.3$), indicating a higher recruitment production rate per unit of biomass compared to the previous stage. Likewise, the biological breakpoint remained at a similar level ($b = 3.16 \cdot 10^5$ t), suggesting stability in the biomass threshold at which saturation occurs (Figure 3.24, left). As a combined result of these parameters, the maximum recruitment plateau (the product $a \cdot b$) increased from approximately $2.67 \cdot 10^6$ to $3.26 \cdot 10^6$ units, confirming a substantial increase in the biological production capacity of the stock during this recent regime. Diagnostic analyses for this period were notably robust, with residuals showing an almost perfect normal distribution (QQ-plot) and no systematic patterns over

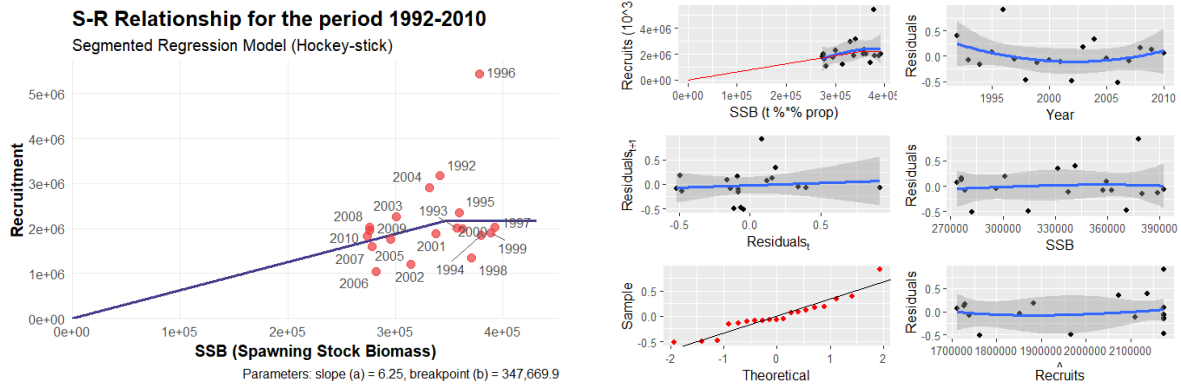


Figure 3.23: Selected model based on AIC and BIC criteria and diagnostic plots for the 1992-2010 period for the horse mackerel in ICES Division 9a. (Left) Hockey-Stick model fit for the horse mackerel across the 1992-2010 period. (Right) Diagnostic plots for the Hockey-Stick model (1992-2010 period) for the horse mackerel in ICES Division 9a.

time. This fit indicated that the stock had consistently operated within the saturation region of the model, maximizing recruitment for the observed biomass levels (Figure 3.24, right).

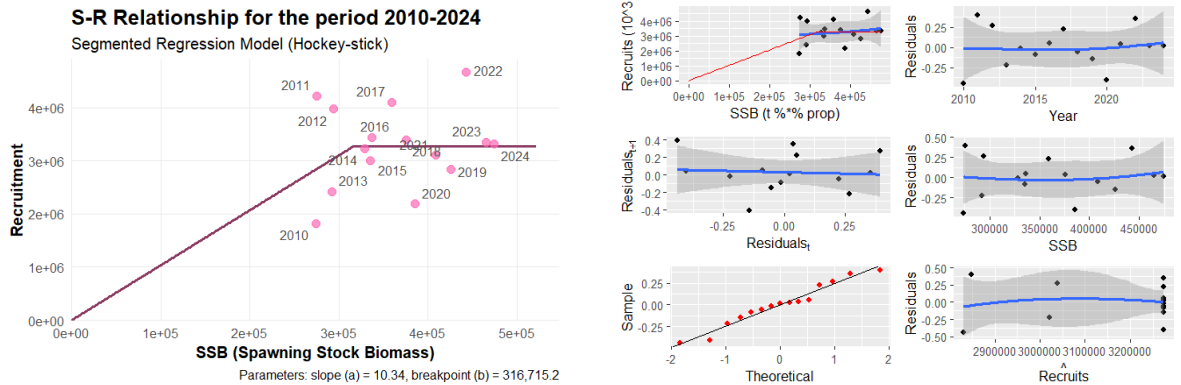


Figure 3.24: Selected model based on AIC and BIC criteria and diagnostic plots for the 2010-2024 period for the horse mackerel in ICES Division 9a. (Left) Hockey-Stick model fit for the horse mackerel across the 2010-2024 period. (Right) Diagnostic plots for the Hockey-Stick model (2010-2024 period) for the horse mackerel in ICES Division 9a.

3.5 Biological Reference Points

The BRPs (Table 3.5) were estimated through stochastic equilibrium simulations using the `msy` (EqSim) package developed by ICES. Uncertainty in the S-R relationship was evaluated by fitting individual Beverton-Holt, Beverton-Holt AR(1), and Hockey-Stick models with the breakpoint fixed at B_{lim} , as well as through model averaging based on smoothed AIC weights following the methodology of Buckland et al. (1997).

Table 3.5: Biological Reference Points obtained through EqSim for the southern horse mackerel (*Trachurus trachurus*) in ICES Division 9a, under different SR relationships.

SR Model	B_{lim}	B_{pa}	$MSY B_{\text{trigger}}$	F_{lim}	F_{pa}	F_{p05}	F_{MSY}
Beverton-Holt	217 497	273 824	273 824	0.111	0.101	0.101	0.057
Beverton-Holt AR(1)	217 497	273 824	273 824	0.110	0.098	0.098	0.058
Buckland (Model Averaging)	217 497	273 824	273 824	0.112	0.101	0.101	0.067
Segreg B_{lim} (Hockey-Stick)	217 497	273 824	273 824	0.160	0.148	0.148	0.117

The segmented regression model with a fixed B_{lim} breakpoint constituted the least conservative approach, as it projects a notably more optimistic fishing collapse threshold ($F_{\text{lim}} = 0.160$) and a higher target fishing mortality ($F_{\text{MSY}} = 0.117$), showing greater convergence with the reference points proposed by WGHANSA (ICES, 2025) (Table 3.6). This tolerance to elevated levels of fishing pressure was grounded in the mathematical structure of the segmented function, since recruitment was assumed to remain constant until the biomass breakpoint (B_{lim}) is strictly reached, thereby omitting any gradual decline in stock productivity at intermediate biomass levels.

According to ICES (2025), MSY is achieved with $F_{\text{MSY}} = 0.115$, providing a catch level of 56520 tonnes and an estimated SSB equal to 520214 tonnes (Table 3.6).

Table 3.6: Estimated biological reference points in WGHANSA (ICES, 2025) for the horse mackerel, in ICES Division 9a.

Reference Point	B_{lim}	B_{pa}	$MSY B_{\text{trigger}}$	F_{lim}	F_{pa}	F_{MSY}	MSY (catch)
Value	201000	279000	279000	0.158	0.146	0.115	520214

In contrast, the Buckland model averaging approach, the Beverton-Holt model, and the Beverton-Holt AR(1) model adopted a more precautionary framework, resulting in considerably more restrictive F_{MSY} values (0.067, 0.057, and 0.058, respectively). The inclusion of first-order autocorrelation allowed temporal dependence in recruitment anomalies to be modeled, which is commonly associated with multiyear fluctuations in environmental regimes. This penalized overly optimistic scenarios and forced the stochastic simulator to adopt a more conservative strategy in order to prevent stock collapse.

It is noteworthy that all configurations evaluated with EqSim strictly complied with the ICES precautionary criteria. In all analyzed cases, the fishing mortality associated with a probability of less than 5% of the stock falling below B_{lim} (F_{p05}) was systematically higher than the fishing mortality estimated for maximum sustainable yield (F_{MSY}). This confirmed that the proposed exploitation rates did not compromise long-term biological sustainability.

The results obtained through FLBRP (Table 3.7) allowed us to examine the behaviour of the southern horse mackerel stock in ICES Division 9.a under a strictly deterministic and static equilibrium framework. Unlike dynamic simulations, FLBRP algebraically computed how biomass, recruitment, and catches would behave if biological conditions remained completely stable over the long term. Under the classical Beverton-Holt model, the virgin SSB (SSB_0 in the unfished state) was $4.30 \cdot 10^6$ tonnes and a baseline recruitment of $1.40 \cdot 10^7$ individuals. Once fishing pressure was introduced, the model placed a $F_{\text{MSY}} = 0.050$ similar to the value obtained with EqSim, which provided a MSY catch level of $7.47 \cdot 10^4$ tonnes. At this exploitation level, SSB was reduced to $1.73 \cdot 10^6$ tonnes, corresponding to approximately 40% of the unfished biomass (B_0). However, the most critical aspect

revealed by FLBRP for this model is the stock sensitivity under increased fishing pressure: if fishing mortality doubled from 0.050 to 0.110, the deterministic collapse threshold (F_{crash}) would be reached immediately.

In contrast, incorporating the Beverton-Holt AR(1) model produced a lower SSB_0 estimate of $8.28 \cdot 10^5$ tonnes with a corresponding recruitment level of $2.69 \cdot 10^6$ individuals. Despite these lower estimates of stock size and productivity, the modified curvature of the stock–recruitment relationship shifted the optimum towards higher fishing mortality levels. F_{MSY} increased to 0.075 but with a substantially lower maximum yield ($2.03 \cdot 10^4$ tonnes). Similarly, the collapse threshold (F_{crash}) increased to 0.172. This implied that under the autoregressive model the stock is perceived as a smaller and less productive population in terms of biomass output, yet mathematically more resilient to higher exploitation rates before the collapse occurs.

For both stock-recruitment models, the estimated values of $F_{0.1}$ and F_{max} were 0.179 and 0.436, respectively. However, when attempting to calculate equilibrium yield, recruitment, and biomass at these fishing mortality levels, no biological feasible equilibrium solution could be obtained. This occurred because $F_{0.1}$ and F_{max} were originally estimated in isolation from yield-per-recruit curves, which implicitly assumed that recruitment was infinite and independent of adult stock size. These results therefore provided quantitative evidence that neither $F_{0.1}$ nor F_{max} are biologically applicable or safe for the management of this stock.

Table 3.7: Biological reference points calculated analytically through FLBRP for southern horse mackerel (*Trachurus trachurus*) in ICES Division 9.a under Beverton-Holt and Beverton-Holt AR(1) stock-recruitment models.

Modelo SR	Reference Point	F (harvest)	Yield	Recruitment	SSB
Beverton-Holt	virgin	0,000	0,00	$1,40 \cdot 10^7$	$4,30 \cdot 10^6$
	msy	0,050	$7,47 \cdot 10^4$	$8,74 \cdot 10^6$	$1,73 \cdot 10^6$
	crash	0,110	0,00	0,00	0,00
BevHolt AR(1)	virgin	0,000	0,00	$2,69 \cdot 10^6$	$8,28 \cdot 10^5$
	msy	0,075	$2,03 \cdot 10^4$	$1,83 \cdot 10^6$	$2,97 \cdot 10^5$
	crash	0,172	0,00	0,00	0,00

3.6 Sensitivity analysis

3.6.1 Steepness

We tested a range of values for the steepness parameter h , identifying $h = 0.55$ as the global optimum value, as it maximized the goodness of fit through the simultaneous minimization of the $\text{AIC} = 36.37$, the $\text{BIC} = 40.86$, and the $\text{RMSE} = 1026.71$, as shown in Table 3.8. Model performance became progressively worse as steepness increases toward values close to 1, although the difference relative to the scenario of highest biological resilience ($h = 0.95$) is only $\Delta\text{AIC} = 1.60$.

This discrepancy between the empirical results and the existing literature may be due to a lack of contrast in the data. In Figure 3.25, the scatterplot was concentrated at high biomass values, while information on stock behavior at low spawning-stock levels is lacking. Under these circumstances, the model was poorly informed about the shape of the S-R relationship near the origin and relied on

the central portion of the curve. Then it effectively linearized the trajectory of the curve within the observed central region at the expense of imposing a biologically restrictive slope near the origin.

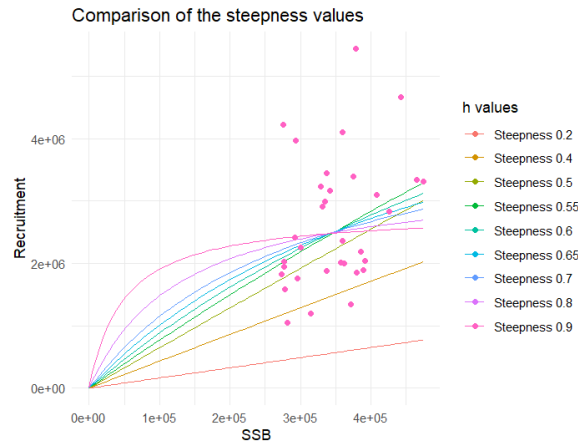


Figure 3.25: Sensitivity analysis of the steepness parameter (h) in the Beverton-Holt model for the S-R relationship of horse mackerel in ICES Division 9.a. The colored lines represent the fitted trajectories for different fixed values of h (ranging from 0.2 to 1.0).

3.6.2 Virgin recruitment

The sensitivity analysis of the Beverton-Holt model to variations in virgin recruitment (R_0) revealed severe parameter uncertainty. The maximum difference observed in the AIC and BIC across the tested range ($0.5 \cdot R_0$ to $1.5 \cdot R_0$) was only $\Delta\text{AIC} = 0.0683$, a value far below the commonly accepted critical threshold of $\Delta\text{AIC} < 2$ (Table 3.8). This suggested that, due to the lack of informative contrast in the data (namely the absence of observations at critical biomass saturation levels), the algorithm compensated for forced increases in the asymptotic ceiling of the curve (a) through proportional increases in the density-dependence parameter (b), thereby preserving an almost identical trajectory within the observed biomass range. Consequently, the absolute value of R_0 could not be estimated with precision using the current time series. As shown in Figure 3.26, the model was unable to estimate the absolute carrying capacity of the stock because all fitted curves followed virtually the same trajectory over the observed data.

3.6.3 Density-dependent effects

The sensitivity analysis of the shape parameter γ in the Shepherd model revealed a scenario similar to that observed for R_0 across the evaluated range of values ($\gamma = 0.5$ to $\gamma = 4.0$). Although the statistical criteria allowed the identification of a global optimum under a scenario of attenuated density dependence ($\gamma = 0.5$; $\text{AIC} = -44.7335$; $\text{BIC} = -41.7405$) (Table 3.8), the likelihood gradient was effectively negligible, with a maximum deviation of only $\Delta\text{AIC} = 0.0779$ relative to the most extreme scenario ($\gamma = 4.0$). This absence of statistical contrast ($\Delta\text{AIC} \ll 2$) confirmed that the horse mackerel time series lacked the structural information required to reveal density-dependent effects at the observed levels of SSB . The convergence toward values of $\gamma < 1.0$ could be explained by the concave and quasi-linear geometry of the observed cloud of points, which does not exhibit signs of asymptotic saturation or reproductive collapse driven by cannibalism.

The visual analysis of the Shepherd model fit (Figure 3.27) corroborated the lack of informative contrast in the time series, as evidenced by the almost complete geometric overlap of the evaluated trajectories within the range of available observations.

Table 3.8: Results of the sensitivity analysis for the parameters of the S-R models (Beverton-Holt and Shepherd) applied to horse mackerel in ICES Division 9.a. The globally optimal scenarios for each analyzed parameter are highlighted in bold.

Model	Parameter	Value	AIC	BIC	RMSE
<i>Beverton-Holt</i>	h	0.20	127.85	132.34	2 320 841.69
<i>Beverton-HoltSV</i>	h	0.40	69.32	73.81	1 520 408.85
<i>Beverton-Holt</i>	h	0.50	36.06	40.55	1 061 870.32
<i>Beverton-Holt</i>	h	0.55	32.65	37.14	981 162.11
<i>Beverton-Holt</i>	h	0.60	32.79	37.28	982 973.20
<i>Beverton-Holt</i>	h	0.65	33.17	37.66	988 113.93
<i>Beverton-Holt</i>	h	0.70	33.68	38.17	995 062.20
<i>Beverton-Holt</i>	h	0.80	34.85	39.34	1 011 119.00
<i>Beverton-Holt</i>	h	0.90	36.03	40.52	1 027 437.00
<i>Beverton-Holt</i>	R_0	$1.17 \cdot 10^7$	-46.66	-45.16	983 117.70
<i>Beverton-Holt</i>	R_0	$1.88 \cdot 10^7$	-46.72	-45.22	981 435.00
<i>Beverton-Holt</i>	R_0	$2.35 \cdot 10^7$	-46.72	-45.23	981 133.40
<i>Beverton-Holt</i>	R_0	$2.82 \cdot 10^7$	-46.72	-45.23	980 992.90
<i>Beverton-Holt</i>	R_0	$3.52 \cdot 10^7$	-46.72	-45.22	980 937.10
<i>Shepherd</i>	β	0.10	NaN	NaN	NaN
<i>Shepherd</i>	β	0.50	-44.73	-41.74	981 065.00
<i>Shepherd</i>	β	0.80	-44.73	-41.74	981 100.70
<i>Shepherd</i>	β	1.00	-44.72	-41.73	981 120.70
<i>Shepherd</i>	β	1.70	-44.71	-41.72	981 204.50
<i>Shepherd</i>	β	2.50	-44.66	-41.66	981 238.60
<i>Shepherd</i>	β	4.00	-44.66	-41.66	981 233.10

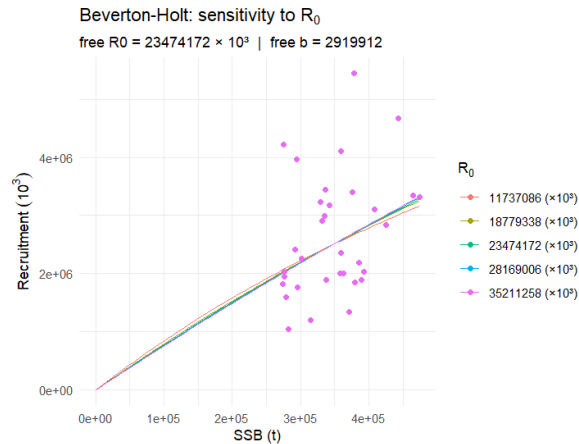


Figure 3.26: Sensitivity analysis of the virgin recruitment parameter (R_0) in the Beverton-Holt model for the S-R relationship of horse mackerel in ICES Division 9.a. The colored lines represent the fitted trajectories for different fixed values of R_0 .

3.6.4 Calculus of the reference points using an alternative steepness

Next, two alternative configurations in Stock Synthesis (SS3) were implemented, using an underlying Beverton-Holt model (analogous to the one previously applied) while modifying the steepness parameter. First, SS3 was run by deterministically fixing steepness at $h = 0.55$. Second, the model structure was relaxed by allowing steepness to be freely estimated from the empirical data series, which yielded an estimate of $h = 0.60$. Comparing these results with the historical base model (with $h = 0.81$) revealed an upward scaling in the temporal trajectories of absolute SSB and recruitment, a necessary adjustment to justify the extraction associated with the historical catches recorded. This, in turn, resulted in systematically lower estimates of F . Comparative graphics of this new runs can be found at [Annex B](#) of the base model (initial run with $h = 0.81$), fixing the steepness at $h = 0.55$ and letting h be freely estimated.

In order to quantify the impact of these new demographic structures on long-term exploitation strategies, I recalculated the set of biological reference points using EqSim, employing both the Beverton-Holt stock-recruitment relationship and a segmented regression model with a breakpoint fixed at B_{lim} . The results are presented in [Table 3.9](#).

Under the lower productivity scenario ($h = 0.55$), the Beverton-Holt model estimated $F_{MSY} = 0.072$ and $F_{lim} = 0.109$. For the scenario with $h = 0.60$, the reference points decreased to $F_{MSY} = 0.053$ and $F_{lim} = 0.099$.

For $h = 0.55$, the Segreg B_{lim} model produced $F_{MSY} = 0.091$ and $F_{lim} = 0.135$, whereas for $h = 0.60$, F_{MSY} and F_{lim} remained almost equal, being 0.092 and 0.139. Consistent with the previous simulations, the hockey-stick-type model, which assumed constant maximum recruitment immediately above the breakpoint, continued to generate substantially more optimistic and less precautionary projections than the Beverton-Holt model.

It is also noteworthy that, across all four simulations conducted, the target fishing mortality (F_{MSY}) consistently remained below its corresponding precautionary filter (F_{p05}).

A low h value drastically reduced the slope of the S-R curve near the origin, implying that the stock is biologically very fragile at low biomass levels. To prevent stochastic fluctuations from driving the population below the newly elevated B_{lim} thresholds, the simulator was forced to strongly restrict both the optimal fishing mortality (F_{MSY}) and the fishing-collapse threshold (F_{lim}).

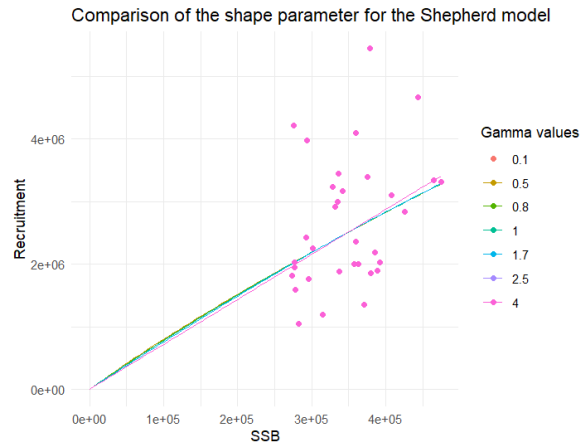


Figure 3.27: Sensitivity analysis of the shape parameter (γ) in the Shepherd model for the S-R relationship of horse mackerel in ICES Division 9.a. The colored lines represent the fitted trajectories for different fixed values of γ , ranging from 0.1 to 4.

Table 3.9: Biological reference points for biomass and fishing mortality estimated using *EqSim* for southern horse mackerel (ICES Division 9a) under different steepness (h) scenarios and S-R models.

SR model	MSY B_{trigger}	B_{pa}	B_{lim}	F_{pa}	F_{lim}	F_{p05}	F_{MSY}
BH $h = 0.5$	284636	284636	226085	0.087	0.109	0.087	0.072
BH $h = 0.6$	272916	272916	216776	0.091	0.099	0.091	0.053
Segreg B_{lim} $h = 0.55$	284636	284636	226085	0.124	0.135	0.124	0.091
Segreg B_{lim} $h = 0.6$	272916	272916	216776	0.128	0.139	0.128	0.092

Chapter 4

Discussion

Our study analysed the stock-recruitment relationship of southern horse mackerel in ICES Division 9a as a step to improve the current SS3 model, and to support the development of a Management Strategy Evaluation (MSE). To achieve this, an exploratory data analysis was conducted, several SR models were evaluated, uncertainty was quantified through residual bootstrap procedures, and BRPs were estimated using stochastic equilibrium simulations.

The most notable findings included the incorporation of an autoregressive time-series component into the stock-recruitment modelling framework, evidence suggesting a potential productivity regime shift during the last decade towards a more productive stock state, and the results of the sensitivity analyses concerning stock resilience, as represented by the steepness parameter (h).

The underlying S-R relationship applied for this stock was revisited and different SR models were fitted and tested to data. The autoregressive Beverton-Holt AR(1), which provided the best performance according to the AIC and BIC, was an attempt to improve the statistical appropriateness of the current approach to the S-R relationship, by explicitly modelling the time-series structure of the recruitments. It is proposed that ARMA time-series models (or variants thereof) might be contemplated in those cases where sufficiently strong evidence for historical time-series structure is available. From a mathematical modeling perspective, the transition between these formulations represented a shift from an assumption of stochastic independence to one of persistent temporal dependence. This finding was consistent with the results reported by Needle et al. (2003). The implementation of residual bootstrap procedure allowed us to compare the performance of both the Beverton-Holt and the Beverton-Holt AR(1) model, and the projections generated by the AR(1) model produced estimates comparable to those obtained under the traditional approach, while exhibiting lower uncertainty and reduced systematic bias in the bootstrap resampling.

This fact may suggest the influence of environmental drivers on recruitment dynamics, such as water temperature, persistent oceanographic circulation patterns, or food availability, all of which tend to operate over multiannual cycles and may therefore induce temporal autocorrelation in recruitment processes.

In the time series from 1992 to 2024, the stock reached its lowest historical level of spawning-stock biomass (SSB) in 2010. However, from that point onwards, it entered a period of elevated productivity characterised by more frequent and more intense recruitment events. This pattern was consistent with the hypothesis of a shift towards a more productive regime during the last decade. Based on the Wilcoxon test, and the Hockey-Stick models fitted for each separated periods, there was evidence that supports an increase in the biomass and productivity of this stock. This increase suggested that the horse mackerel stock has entered a phase of higher productivity, possibly driven by changes in environmental conditions (Reid et al., 2001).

Although this suggested a transition towards a higher productivity regime in the last decade, more advanced analyses are required to formally confirm the existence of a regime shift, such as the collection of statistical tests described in Rodinov (2005), such as a Student t-test, a Bayesian analysis,

a cumulative deviation test, and others. The ultimate goal in the detection of regime shift should be encouraging management of marine ecosystems that is geared towards developing resilience, as it was suggested in DeYoung et al. (2008)

The estimation of BRPs through equilibrium stochastic simulations with EqSim (Table 3.5) revealed a significant sensitivity with respect to the selected S-R relationship, the Beverton-Holt model with AR(1) error structure. This constituted evidence of that the choice of the subjacent mathematical model is key for simulating long-term projections of the stock, and therefore must be carefully revised, since it has a great impact on the calculation of BRPS, and therefore in achieving MSY .

The Hockey-Stick model (with a breakpoint fixed at B_{lim}) emerged as the least conservative approach ($F_{MSY} = 0.117$), aligning almost perfectly with the current reference points adopted by the ICES WGHANSA working group ($F_{MSY} = 0.115$) during the 2024 benchmark for Atlantic horse mackerel (ICES, 2024) (Table 3.6). The tolerance of this model in EqSim to high levels of fishing pressure was rooted directly in its algebraic formulation: by assuming that recruitment remains constant at its maximum level until spawning biomass declines below B_{lim} , it neglected any gradual reduction in stock productivity at intermediate biomass levels. As a result, the model inherently portrayed the population as being more resilient to exploitation, thereby supporting higher estimates of sustainable fishing mortality.

In contrast, the Beverton-Holt-based models and the model-averaging approach (Buckland) suggested a substantially more restrictive and precautionary management strategy ($F_{MSY} \approx 0.058-0.067$). Adopting the reference points derived from the Beverton-Holt AR(1) model would imply a marked reduction in allowable catches (TACs), prioritizing precaution, whereas maintaining the current ICES approach assumes a stock that is more resilient to fishing pressure.

In contrast to the stochastic dynamics explored using EqSim, the deterministic equilibrium analysis provided by FLBRP (Table 3.7) reveals several notable differences. Under the standard Beverton-Holt model, the stock was characterized by an estimated virgin spawning-stock biomass of SSB_0 , a virgin recruitment level R_0 , and an optimal fishing mortality of F_{MSY} , broadly consistent with the corresponding EqSim estimate. At this exploitation level, the stock stabilized at approximately 40% of its virgin biomass. However, this scenario also highlighted a substantial vulnerability, as a relatively modest increase in fishing mortality to $F = 0.110$ would drive the stock to reach its deterministic collapse threshold (F_{crash}).

The incorporation of an autoregressive error structure through the Beverton-Holt AR(1) model substantially altered the curvature of the S-R function and led to a somewhat counterintuitive interpretation. Under this formulation, the stock was perceived as a considerably smaller population with a lower carrying capacity, exhibiting an estimated SSB_0 and R_0 lower than those obtained under the standard Beverton-Holt model. Nevertheless, the estimated exploitation rate increased ($F_{MSY} = 0.075$), associated with a substantially lower MSY while simultaneously increasing the collapse threshold F_{crash} . These results suggested that incorporating the autoregressive component described a stock supporting a lower equilibrium biomass but mathematically more resilient to elevated levels of fishing mortality.

Finally, the analytical estimates of deterministic reference points that do not explicitly incorporate a S-R relationship, such as $F_{0.1}$ and F_{max} , further demonstrated the limitations of static Yield-per-Recruit (YPR) approaches for the southern horse mackerel stock. Because they did not account for the feedback between spawning biomass and recruitment, they tended to overestimate sustainable fishing mortality and might therefore underestimate the long-term risks associated with stock depletion.

A particularly important result was the divergence observed between the reference points estimated by EqSim and those derived from FLBRP. Whereas FLBRP provided a diagnostic framework based on deterministic and static equilibrium conditions, EqSim implemented a stochastic and dynamic simulation approach. The latter was fully aligned with the MSY framework adopted by ICES (and also supporting PA) for stock assessment and the development of HCRs. The analytical advantages of EqSim became especially evident through its ability to incorporate temporal dependence structures, such as the autoregressive processes examined in this study, providing a more realistic characterization of stock dynamics.

From a fisheries governance and sustainability perspective, the principal limitation of determinis-

tic approaches such as FLBRP lied in their inability to quantify probabilistic risk. Under the ICES precautionary framework, an estimate of F_{MSY} is considered biologically acceptable only if it is associated with less than a 5% probability of the spawning-stock biomass falling below B_{lim} . FLBRP could not evaluate this probability directly and was therefore limited to identifying theoretical collapse thresholds. By contrast, EqSim explicitly computed the precautionary risk indicator F_{p05} by tracking the proportion of simulated trajectories that fall below B_{lim} . Whenever the deterministic optimum exceeded the acceptable risk threshold, fishing mortality was automatically constrained within the simulation framework, thereby ensuring that management advice remained consistent with a probabilistic definition of biological sustainability.

For these reasons, EqSim provided a more suitable basis for the development of operating models and biological reference points for future Management Strategy Evaluation (MSE) analyses of the southern horse mackerel stock. EqSim explicitly incorporated recruitment variability, uncertainty, probabilistic risk, and temporal dependence in stock dynamics, allowing a more realistic representation of population processes and their response to exploitation.

Steepness (h) is a key parameter in statistical catch-at-age stock assessments, and its specification can have major consequences for management actions when it cannot be reliably estimated from the available data. Consequently, steepness is frequently pre-specified in integrated models (Punt and Dorn, 2014). When a fish stock is highly exploited or in data-limited situations, it is common to employ prior information from meta-analysis or another similar species. This practice of fixing h externally arises because available data often lack the informative power to clearly distinguish between widely contrasting values, a limitation previously highlighted by Johnston (2005). As stated in Miller and Brooks (2020), the steepness-based parameterization implicitly assumes that post-recruitment biological conditions, such as weight-at-age, maturity-at-age, and natural mortality, remain constant over time. In real populations, however, these productivity-related parameters often vary substantially in response to environmental fluctuations, ecosystem changes, and anthropogenic pressures. By forcing the model to adopt a single steepness value and a fixed ϕ_0 throughout the entire time series, an inherent misspecification is introduced. As a consequence, the resulting S-R relationship may not accurately reflect the true underlying biological dynamics, potentially leading to a distorted representation of stock productivity and, ultimately, to substantial changes in the estimation of BRPs.

In this study, when steepness was allowed to be freely estimated, either within the sensitivity analysis or the alternative SS3 configurations, the model converged on low values, both being similar (0.55 and 0.6). From a biological standpoint, these estimates would characterize a stock with relatively low resilience. This result meant that if the SSB is reduced to 20% of its virgin level (S_0), the expected recruitment would decrease sharply to only 55% (or 60%) of the virgin recruitment (R_0). This contrasts with the higher steepness values typically expected and employed for small pelagic species such as horse mackerel (ICES, 2024). This implied a structural shift in both the estimated BRPs and the perceived productivity of the stock.

The run with fixed $h = 0.55$ provided a significantly higher SSB estimate than the historical model (Figure 1), compared to the base and the $h = 0.6$. This was due to the fact that a less resilient stock, SS3 incremented the biomass estimation to account for the levels of recruitment and catches observed. It was remarkable the fact that, when allowing h to be freely estimated, SSB behaved similarly to the base model. The confidence intervals remained very similar (Figure 2).

According to the reasoning outlined above, the run with $h = 0.55$ yielded slightly lower estimates of F (Figure 3). Because the model estimated a larger SSB , the same reported catches correspond to a lower exploitation rate.

Recruitment estimates were virtually identical across the three model configurations (Figures 4 and 5). Major recruitment outliers (1996, 2011, 2016, and the recent event in 2022) are reproduced consistently in all runs, indicating that the alternative steepness assumptions had little influence on the reconstruction of recruitment dynamics over the observed period.

The run with fixed steepness also estimated a higher logarithm of R_0 (Figures 6 and 7), with no overlap whatsoever with the other two results. In statistical terms, this implied that the low productivity scenario ($h = 0.55$) required a significantly higher level of virgin recruitment compared

to the other two scenarios, which appeared more similar to each other. Additionally, fixing steepness at $h = 0.55$ yielded a substantially higher estimate of SSB_0 relative to the others (Figures 8 and 9).

This was crucial to explain why the run with lower steepness, which a priori might imply a less resilient stock and greater susceptibility to increases in F , produced more optimistic BRP estimates. Due to the internal structure of SS3, this specification inflated the scale of the stock (R_0 and SSB_0), and when simulations were subsequently run in EqSim, this led to less precautionary scientific advice, with higher and more permissive F thresholds.

In contrast, the run where steepness was freely estimated ($h = 0.60$) maintained a more realistic and biologically coherent stock scale, resulting in more conservative and precautionary BRPs.

Future research should therefore explore the incorporation of an autoregressive component into the underlying S-R relationship within the SS3 framework and investigate how such a modification affects the estimation of steepness. This could provide a more realistic representation of temporal dependence in recruitment dynamics and help determine whether the current steepness estimates are biased by the assumption of independent recruitment deviations.

The results obtained are intended to improve the settings of the stock assessment use to manage southern stock of horse mackerel in ICES Division 9a, and to propose new BRPs. Furthermore, the results could contribute to the development of robust operating models that can subsequently be applied within a MSE framework for horse mackerel management.

Chapter 5

Conclusions

A summary of this work was presented during the most recent meeting of WGHANSA in May 2025 through a Working Document (Puate et al., 2026).

- The comprehensive analysis of the S-R relationship of Southern horse mackerel (*Trachurus trachurus*) in ICES Division 9.a revealed that incorporating a first-order autoregressive (AR(1)) component into the Beverton-Holt model substantially improved statistical fit by mitigating temporal dependence in the residuals.
- The observed autocorrelation was consistent with a period of increased stock productivity and recruitment events since 2010, suggesting that recruitment dynamics were influenced by processes not fully explained by the SSB like environmental drivers.
- The evaluation of BRPs demonstrated that stochastic simulations (EqSim) provided a better framework for management advice than the to static deterministic approaches (FLBRP), primarily because of their ability to rigorously quantify the probabilistic risk required under the ICES precautionary approach.
- Furthermore, the findings call into question the analytical validity of pre-specifying high-resilience parameters (steepness), as unconstrained estimations suggest a lower resilience of the stock than has historically been assumed. Continued reliance, on the SegregB_{tim} model may lead to an overestimation of the stock's tolerance to fishing pressure, highlighting the need to transition towards more conservative S-R formulations that better ensure the long-term sustainability of the resource.

Annex A

Table 1: Main characteristics and settings of the southern horse mackerel assessment model.

Component	Description
Model type	Annual, age-based, single-area assessment model following ICES (2025).
Population structure	Age classes from 0 (recruits) to an aggregated 11+ group; sexes treated indistinctly.
Catch data	Total catches in biomass units and age composition in numbers-at-age.
Abundance indices	Abundance in biomass units with age composition, standardized commercial CPUE in biomass, and <i>SSB</i> estimated from a triennial DEPM survey.
Natural mortality	Age-specific fixed input values.
Weight-at-age	External estimates of weights-at-age at the beginning of the year.
Maturity-at-age	External estimates of maturity-at-age at the beginning of the year.
Assessment period	All available data included up to year y (final year in ICES terminology).
Stock-recruitment relationship	Beverton-Holt model.
Steepness (h)	Fixed at 0.81.
Recruitment variability	Standard deviation of log-recruitment fixed at 0.74, based on analogous species.

Table 2: Definition, purpose and mathematical basis of the standard biological and per-recruit reference points calculated analytically by the FLBRP package in FLR.

FLBRP Reference Point	Definition	Basis / Mathematical Concept
virgin	The theoretical status of the stock in the complete absence of fishing mortality ($F = 0$).	Represents the unexploited carrying capacity. Yield is zero, and recruitment (R) and spawning-stock biomass (SSB) reach their maximum potential levels (B_0).
F_{MSY}	The deterministic fishing mortality rate that maximizes long-term yield.	The peak of the equilibrium yield curve. Unlike EqSim, it is derived analytically from the deterministic intersection of the growth/selectivity vectors and the stock-recruitment model, without stochastic constraints (F_{p05}).
F_{crash}	The theoretical exploitation rate that leads the stock to complete extinction.	The fishing mortality rate at which the slope of the yield-per-recruit curve at the origin equals the inverse of the slope of the stock-recruitment relationship at the origin. If $F > F_{crash}$, the stock cannot sustain itself.
Per-Recruit Proxy	Purpose	Basis (Independent of Recruitment)
$F_{0.1}$	A traditional conservative proxy for F_{MSY} used when stock-recruitment data is highly uncertain.	The fishing mortality rate at which the marginal increase in yield per recruit (YPR) is exactly 10% of the marginal increase in YPR in an unexploited stock ($F = 0$).
F_{max}	The fishing mortality rate that maximizes the growth potential of a cohort.	The peak of the yield-per-recruit curve. It ignores recruitment failure, assuming that recruitment is constant and entirely independent of parent stock size (SSB).
$F_{30\%SPR}$	A spawning biomass-based proxy used to protect the reproductive potential from recruitment overfishing.	The fishing mortality rate that reduces the Spawning Potential Ratio (SPR , or SSB per recruit) to exactly 30% of its unexploited level (virgin SPR).

Annex B

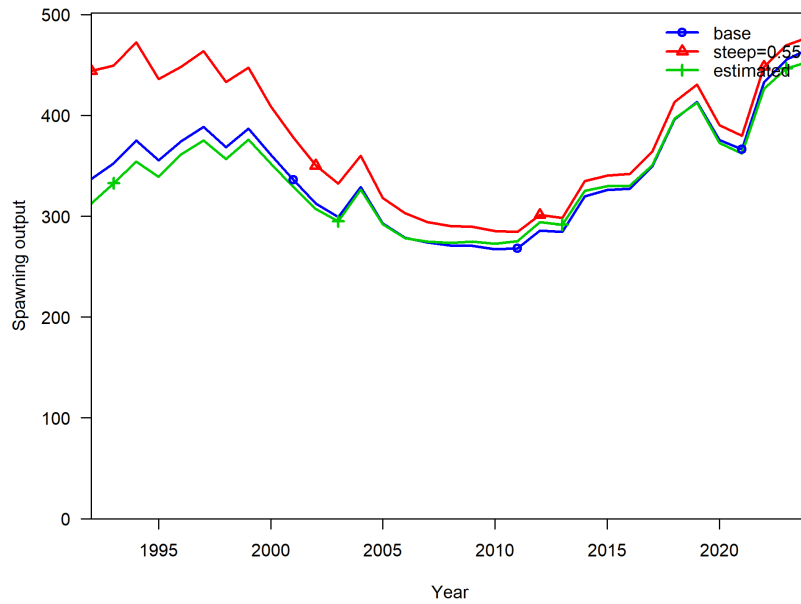


Figure 1: Comparison of the 1992–2024 time series of SSB estimates for Southern horse mackerel obtained using Stock Synthesis (SS3) under three different *steepness* (h) scenarios: the ICES base case ($h = 0.81$, blue line), fixed empirical optimal steepness ($h = 0.55$, red line), and freely estimated steepness ($h = 0.60$, green line).

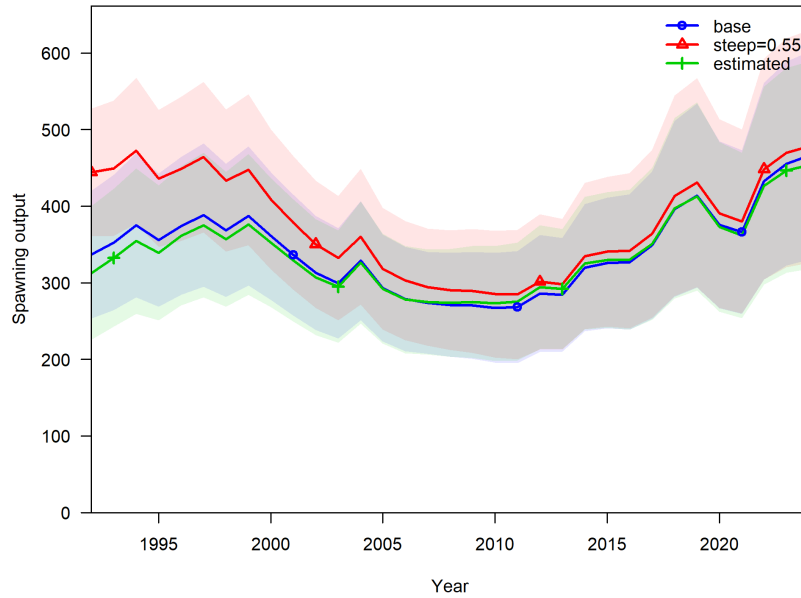


Figure 2: Historical trajectories of SSB with their corresponding 95% confidence intervals (shaded bands) for the three steepness scenarios analysed in SS3 for Southern horse mackerel in ICES Division 9a.

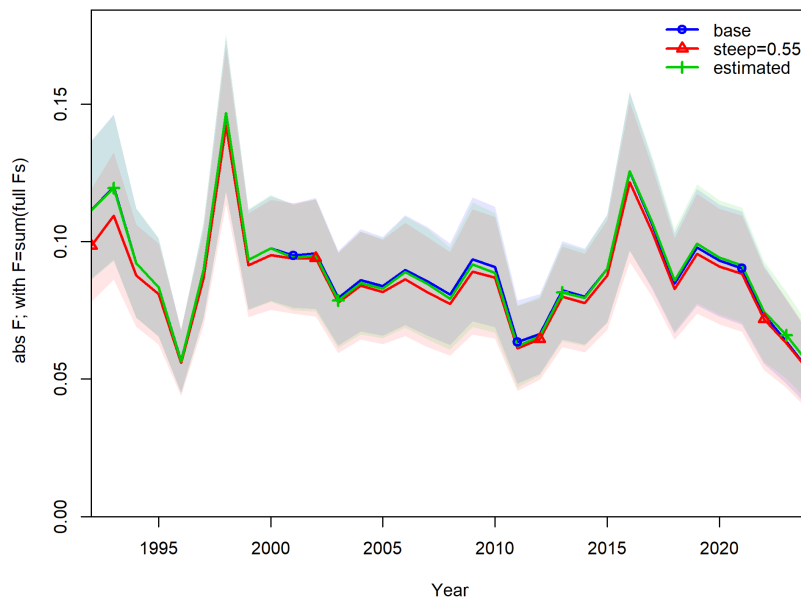


Figure 3: Fishing mortality (F) with their corresponding 95% confidence intervals (shaded bands) trajectories estimated for Southern horse mackerel between 1992 and 2024 under the three tested steepness scenarios for ICES Division 9a.

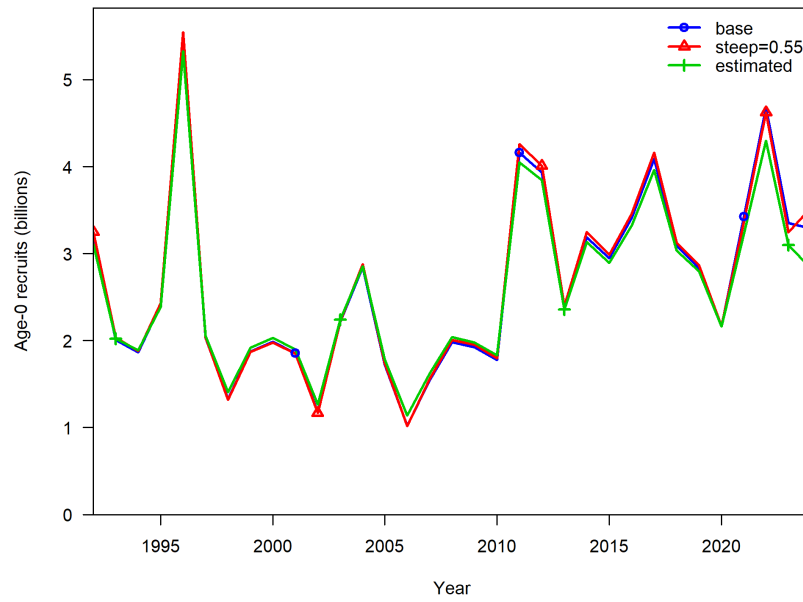


Figure 4: Historical recruitment estimates (Age-0 recruits) in number of individuals for Southern horse mackerel under the three steepness scenarios for ICES Division 9a.

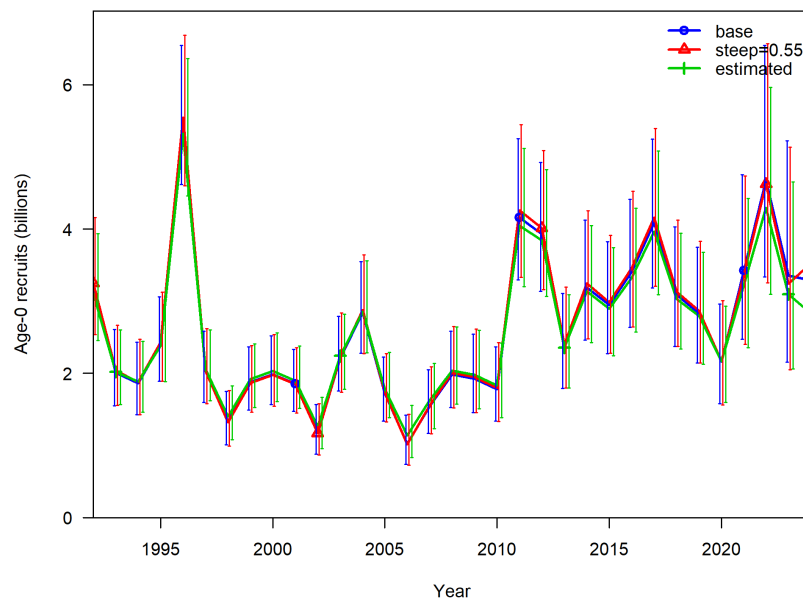


Figure 5: Historical recruitment estimates (Age-0 recruits) with 95% confidence intervals in number of individuals for Southern horse mackerel under the three scenarios for ICES Division 9a.

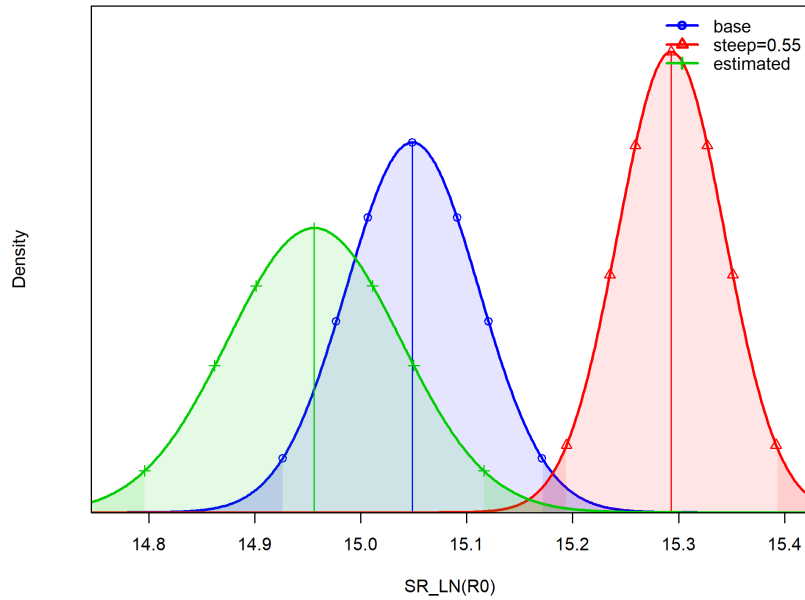


Figure 6: Probability density functions (PDFs) of the natural logarithm of virgin recruitment $[\ln(R_0)]$ estimated by SS3 under the three steepness scenarios for the Southern horse mackerel in ICES 9a.

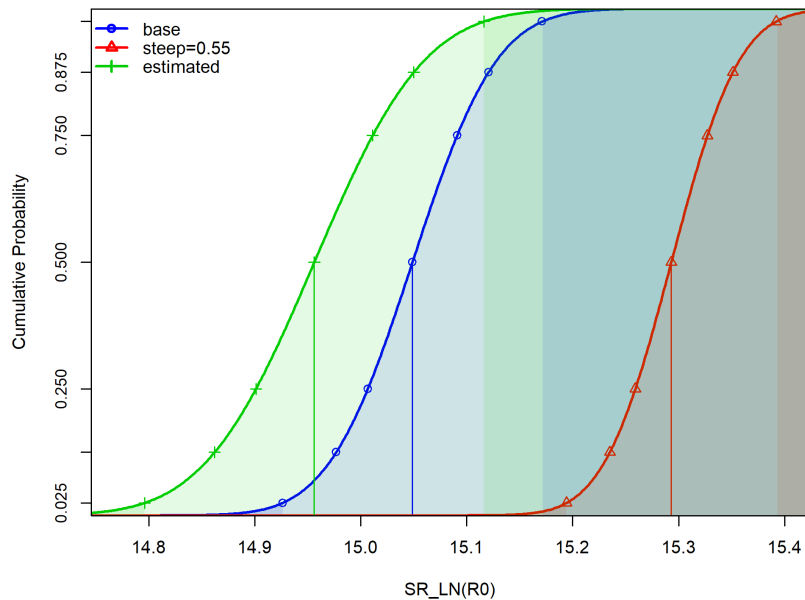


Figure 7: Cumulative distribution functions (CDFs) of the parameter $\ln(R_0)$ for the three steepness scenarios analysed in SS3 for the Southern horse mackerel in ICES 9a.

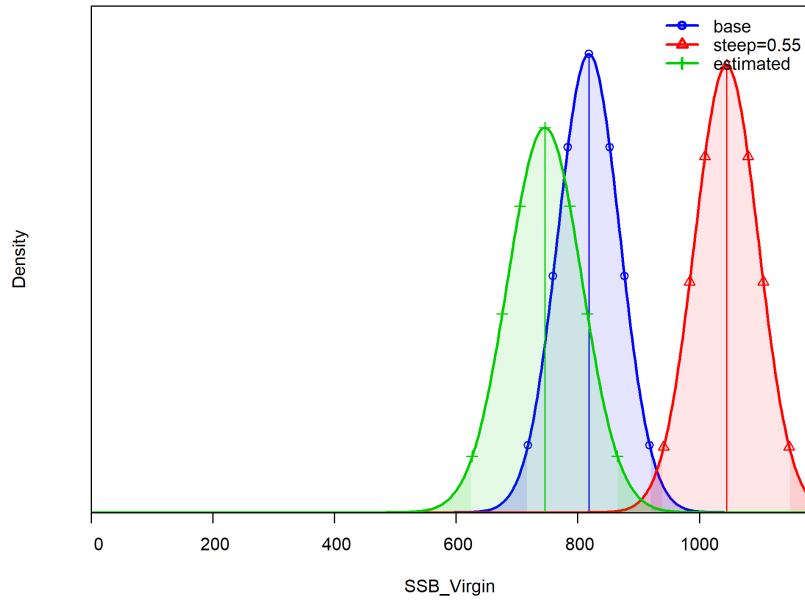


Figure 8: Probability density functions (PDFs) of the SSB_0 estimated by SS3 under the three steepness scenarios for the Southern horse mackerel in ICES 9a.

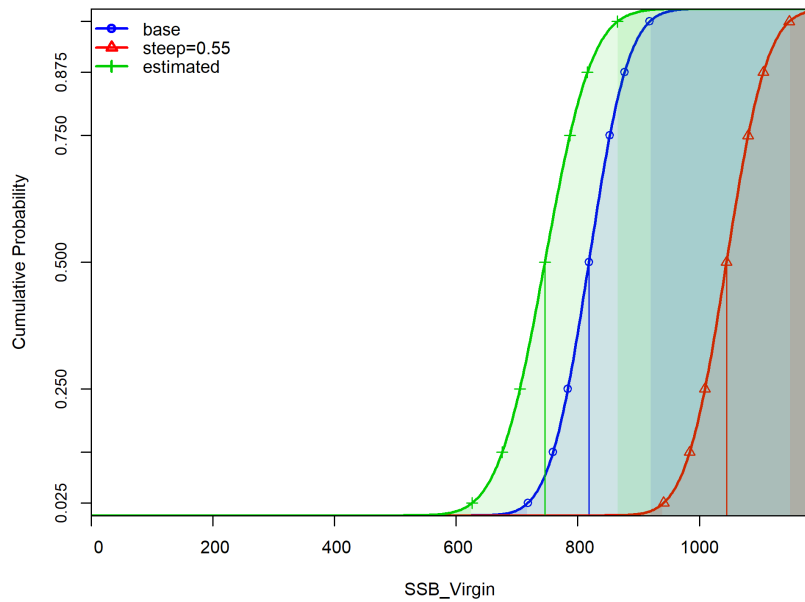


Figure 9: Cumulative distribution functions (CDFs) of the SSB_0 estimated for the three steepness scenarios analysed in SS3 for the Southern horse mackerel in ICES 9a.

List of Figures

1	Map of ICES' Sub-areas and divisions in the North East Atlantic.	xiv
1.1	Southern horse mackerel (<i>Trachurus trachurus</i>).	3
1.2	Stocks of horse mackerel and distribution across the Northeast Atlantic.	3
1.3	Catch trends for the Southern horse mackerel in ICES Division 9a.	4
2.1	Statistical subdivisions within ICES Division 9a.	5
2.2	Time series of <i>SSB</i> levels between 1992 and 2024.	6
2.3	Time series of recruitment levels between 1992 and 2024.	7
2.4	Caption	7
2.5	Beverton-Holt model curve.	10
2.6	Ricker model curve.	11
2.7	Hockey-Stick model curve.	12
2.8	Harvest Control Rule (HCR) established by ICES.	15
3.1	Scatter plot of <i>SSB</i> vs. recruitment with linear fit for the horse mackerel in ICES Division 9a.	23
3.2	Diagnostic plots for the fitted linear regression model. (I) Residuals vs Fitted values. (II) Normal Q-Q plot of residuals. (III) Scale-Location plot. (IV) Residuals vs Leverage plot.	24
3.3	Plot of <i>SSB</i> vs. recruitment with log-log fit for the horse mackerel in ICES Division 9a.	24
3.4	Partial smooth effect of $s(SSB)$ on the logarithm of recruitment. The central curve illustrates the spline estimated by the GAM, the shaded band represents the 95% confidence interval, and the points distributed along the curve represent the partial residuals of the model.	25
3.5	Diagnostic plots for the fitted generalized additive model (GAM). (I) Smooth term plot for the predictor <i>SSB</i> , showing the estimated non-linear effect together with confidence bands and partial residuals. (II) Q-Q plot of deviance residuals. (III) Residuals versus linear predictor. (IV) Histogram of residuals.	25
3.6	Pairs plot of the distribution of <i>SSB</i> and recruitment for the horse mackerel in years 1992-2024 in ICES Division 9a.	26
3.7	Autocorrelation function of recruitment for the horse mackerel in years 1992-2024 in ICES Division 9a.	26
3.8	Beverton-Holt S-R model fit for Southern horse mackerel in ICES 9a and showing the slope at the origin.	27
3.9	Stock-recruit FLR summary plot for Beverton-Holt model. (I) Fitted and observed relationship; (II) residuals-by-year; (III) autocorrelation trend (slope of line) in the residuals; (IV) residuals-by- <i>SSB</i> ; (V) qq-plot of residuals and confidence intervals; (VI) residuals-by-predicted recruitment.	28

3.10	Ricker S-R model fit for Southern horse mackerel in ICES 9a and showing the slope at the origin.	29
3.11	Stock-recruit FLR summary plot for Ricker model. (I) Fitted and observed relationship; (II) residuals-by-year; (III) autocorrelation trend (slope of line) in the residuals; (IV) residuals-by-SSB; (V) qq-plot of residuals and confidence intervals; (VI) residuals-by-predicted recruitment.	30
3.12	Hockey-Stick S-R model fit for Southern horse mackerel in ICES 9a and showing the slope at the origin.	31
3.13	Stock-recruit FLR summary plot for Hockey-Stick model. (I) Fitted and observed relationship; (II) residuals-by-year; (III) autocorrelation trend (slope of line) in the residuals; (IV) residuals-by-SSB; (V) qq-plot of residuals and confidence intervals; (VI) residuals-by-predicted recruitment.	32
3.14	Beverton-Holt AR(1) S-R model fit for Southern horse mackerel in ICES 9a and showing the slope at the origin.	33
3.15	Model comparison between Beverton-Holt (red) and Beverton-Holt AR(1) S-R model (purple) fit for Southern horse mackerel in ICES 9a.	34
3.16	Stock-recruit FLR summary plot for Beverton-Holt AR(1) model. (I) Fitted and observed relationship; (II) residuals-by-year; (III) autocorrelation trend (slope of line) in the residuals; (IV) residuals-by-SSB; (V) qq-plot of residuals and confidence intervals; (VI) residuals-by-predicted recruitment.	35
3.17	Comparison of stock-recruitment models for the horse mackerel in ICES Division 9a: Ricker (cyan), Beverton-Holt (red), Hockey-Stick (purple), and Beverton-Holt AR(1) (green).	37
3.18	Bootstrap distributions of the parameters of the standard Beverton-Holt model ($n = 2000$). (Left) Bootstrap distribution parameter a (productivity). (Right) Bootstrap distribution of parameter b (saturation) for the B-H model.	37
3.19	Bootstrap distributions of the parameters of the Beverton-Holt AR(1) model. (Upper, left) Distribution of parameter a . (Upper, right) Distribution of parameter b . (Below) Distribution of parameter ρ	39
3.20	Boxplot of recruitment for the horse mackerel in ICES 9a across years 1992-2024, separated in two different time series (1992-2010 and 2010-2024).	40
3.21	Recruitment time series for the horse mackerel in ICES Division 9a, separating the first period (1992- 2010, in blue) and the second (2010- 2024, in red).	41
3.22	SSB time series, separating the first period (blue) and the second (red).	41
3.23	Selected model based on AIC and BIC criteria and diagnostic plots for the 1992-2010 period for the horse mackerel in ICES Division 9a. (Left) Hockey-Stick model fit for the horse mackerel across the 1992-2010 period. (Right) Diagnostic plots for the Hockey-Stick model (1992-2010 period) for the horse mackerel in ICES Division 9a.	42
3.24	Selected model based on AIC and BIC criteria and diagnostic plots for the 2010-2024 period for the horse mackerel in ICES Division 9a. (Left) Hockey-Stick model fit for the horse mackerel across the 2010-2024 period. (Right) Diagnostic plots for the Hockey-Stick model (2010-2024 period) for the horse mackerel in ICES Division 9a.	42
3.25	Sensitivity analysis of the steepness parameter (h) in the Beverton-Holt model for the S-R relationship of horse mackerel in ICES Division 9.a. The colored lines represent the fitted trajectories for different fixed values of h (ranging from 0.2 to 1.0).	45
3.26	Sensitivity analysis of the virgin recruitment parameter (R_0) in the Beverton-Holt model for the S-R relationship of horse mackerel in ICES Division 9.a. The colored lines represent the fitted trajectories for different fixed values of R_0	47
3.27	Sensitivity analysis of the shape parameter (γ) in the Shepherd model for the S-R relationship of horse mackerel in ICES Division 9.a. The colored lines represent the fitted trajectories for different fixed values of γ , ranging from 0.1 to 4.	48

1	Comparison of the 1992–2024 time series of SSB estimates for Southern horse mackerel obtained using Stock Synthesis (SS3) under three different <i>steepness</i> (h) scenarios: the ICES base case ($h = 0.81$, blue line), fixed empirical optimal steepness ($h = 0.55$, red line), and freely estimated steepness ($h = 0.60$, green line).	57
2	Historical trajectories of SSB with their corresponding 95% confidence intervals (shaded bands) for the three steepness scenarios analysed in SS3 for Southern horse mackerel in ICES Division 9a.	58
3	Fishing mortality (F) with their corresponding 95% confidence intervals (shaded bands) trajectories estimated for Southern horse mackerel between 1992 and 2024 under the three tested steepness scenarios for ICES Division 9a.	58
4	Historical recruitment estimates (Age-0 recruits) in number of individuals for Southern horse mackerel under the three steepness scenarios for ICES Division 9a.	59
5	Historical recruitment estimates (Age-0 recruits) with 95% confidence intervals in number of individuals for Southern horse mackerel under the three scenarios for ICES Division 9a.	59
6	Probability density functions (PDFs) of the natural logarithm of virgin recruitment [$\ln(R_0)$] estimated by SS3 under the three steepness scenarios for the Southern horse mackerel in ICES 9a.	60
7	Cumulative distribution functions (CDFs) of the parameter $\ln(R_0)$ for the three steepness scenarios analysed in SS3 for the Southern horse mackerel in ICES 9a.	60
8	Probability density functions (PDFs) of the SSB_0 estimated by SS3 under the three steepness scenarios for the Southern horse mackerel in ICES 9a.	61
9	Cumulative distribution functions (CDFs) of the SSB_0 estimated for the three steepness scenarios analysed in SS3 for the Southern horse mackerel in ICES 9a.	61

List of Tables

2.1	The definition and basis of precautionary approach (PA) and MSY reference points used by ICES to assess the state of stocks and exploitation.	17
2.2	EqSim settings used in simulation to determine reference points for horse mackerel.	18
3.1	Estimated parameters for the fitted SR models for the horse mackerel in ICES 9a, from 1992-2024.	36
3.2	Comparison of information criteria (AIC and BIC) for the evaluated stock-recruitment models.	36
3.3	Residual bootstrap confidence intervals ($n = 2000$) for the Beverton-Holt model parameters.	38
3.4	Residual bootstrap results for the Beverton-Holt model with $AR(1)$ structure.	38
3.5	Biological Reference Points obtained through EqSim for the southern horse mackerel (<i>Trachurus trachurus</i>) in ICES Division 9a, under different SR relationships.	43
3.6	Estimated biological reference points in WGHANSA (ICES, 2025) for the horse mackerel, in ICES Division 9a.	43
3.7	Biological reference points calculated analytically through FLBRP for southern horse mackerel (<i>Trachurus trachurus</i>) in ICES Division 9.a under Beverton-Holt and Beverton-Holt $AR(1)$ stock-recruitment models.	44
3.8	Results of the sensitivity analysis for the parameters of the S-R models (Beverton-Holt and Shepherd) applied to horse mackerel in ICES Division 9.a. The globally optimal scenarios for each analyzed parameter are highlighted in bold.	46
3.9	Biological reference points for biomass and fishing mortality estimated using <i>EqSim</i> for southern horse mackerel (ICES Division 9a) under different steepness (h) scenarios and S-R models.	48
1	Main characteristics and settings of the southern horse mackerel assessment model.	55
2	Definition, purpose and mathematical basis of the standard biological and per-recruit reference points calculated analytically by the FLBRP package in FLR.	56

Glossary

ACF Autocorrelation Function.

BRP Biological Reference Point(s), a set of biological indicators established to assess stock status and its response to fishing pressure, along with precautionary limits that represent risk thresholds for stock sustainability.

EqSim Stochastic Equilibrium Reference Point Software.

F Fishing mortality, the instantaneous rate at which individuals are removed due to fishing activity.

FLR Fisheries Library in R, an open and collaborative software framework, including a collection of tools for fisheries science developed in R, designed for building simulations of fisheries models.

GAM Generalized Additive Model.

ICES International Council for the Exploration of the Sea.

MSY Maximum Sustainable Yield, the maximum long-term average yield that can be taken from a fish stock while maintaining its productivity.

PA Precautionary Approach, precautionary thresholds intended to reduce the risk of stock depletion and as proxies to avoid exceeding critical stock states.

SLR Simple Linear Regression.

SSB Spawning Stock Biomass, the biomass of mature individuals capable of contributing to reproduction.

S-R Relationship Stock-recruitment relationship, empirical relationship between *SSB* and the subsequent recruitment of the year class produced by that spawning event.

TAC Total Allowable Catches.

WGHANSA Working Group on Southern horse mackerel, anchovy and sardine.

Bibliography

- [1] Azevedo M, Mendes H, Costas G, Jardim E, Mosqueira I, Scott F (2017) Long-Term Management Strategy for Southern Horse Mackerel (hom27.9a) - Management Strategy Evaluation. Relatórios Científicos e Técnicos do IPMA 19.
- [2] Barrowman NJ, Myers RA (2000) Still more spawner-recruitment curves: the hockey stick and its generalisations. *Canadian Journal of Fisheries and Aquatic Sciences* 57:665-676.
- [3] Beverton RJH, Holt SJ (1957) On the Dynamics of Exploited Fish Populations (Fishery Investigations, Series II, Vol. XIX). Ministry of Agriculture, Fisheries and Food, Great Britain.
- [4] Begg GA, Friedland KD, Pearce JB (1999) Stock identification and its role in stock assessment and fisheries management: an overview. *Fisheries Research* 43:1-8.
- [5] Box GEP, Jenkins GM (1976) *Time Series Analysis: Forecasting and Control*, 2nd edn. Holden-Day, San Francisco.
- [6] Buckland ST, Burnham KP, Augustin NH (1997) Model selection: an integral part of inference. *Biometrics* 53:603-618.
- [7] Cao Abad R, Fernández Casal R (2022) Técnicas de Remuestreo. Apuntes de la asignatura.
- [8] Carvalho F, Winker H, Courtney D, Kapur M, Kell L, Cardinale M, Methot RD (2021) A cookbook for using model diagnostics in integrated stock assessments. *Fisheries Research* 240:105959.
- [9] Cebrián JL, Costas G, Mendes H (2025) Horse mackerel (*Trachurus trachurus*) in Division 9.a (Atlantic Iberian waters). ICES Stock Annex. ICES, International Council for the Exploration of the Sea.
- [10] Courchamp F, Berec L, Gascoigne J (2008) *Allee Effects in Ecology and Conservation*. Oxford University Press, Oxford.
- [11] Cousido-Rocha M, Pennino MG, Izquierdo F, Paz A, Lojo D, Tifoura A, Cerviño S (2022) Surplus production models: a practical review of recent approaches. *Reviews in Fish Biology and Fisheries* 17:1085-110.
- [12] Cushing DH (1973) Dependence of recruitment on parent stock. *Journal of the Fisheries Research Board of Canada* 30:1965-1976.
- [13] Deriso RB (1980) Harvesting strategies and parameter estimation for an age-structured model. *Canadian Journal of Fisheries and Aquatic Sciences* 37:268-282.
- [14] DeYoung B, Barange M, Beaugrand G, Harris R, Perry RI, Scheffer M, Werner F (2008) Regime shifts in marine ecosystems: detection, prediction and management. *Trends in Ecology & Evolution* 23:402-409.
- [15] FAO (1995) *Code of Conduct for Responsible Fisheries*. FAO, Rome.

- [16] FAO (2024) The State of World Fisheries and Aquaculture 2024: Blue Transformation in action. FAO, Rome.
- [17] FAO-FIGIS (2005) A world overview of species of interest to fisheries. Chapter: *Trachurus trachurus*. FIGIS Species Fact Sheets. Species Identification and Data Programme-SIDP, FAO-FIGIS. <http://www.fao.org/figis/servlet/species?fid=2306>. Accessed 05 May 2005.
- [18] Haddon M (2011) Modelling and Quantitative Methods in Fisheries, 2nd edn. Chapman & Hall/CRC, Boca Raton.
- [19] Hilborn R, Walters CJ (1992) Quantitative Fisheries Stock Assessment: Choice, Dynamics and Uncertainty. Chapman & Hall, London.
- [20] Hillary R (2009) An introduction to FLR fisheries simulation tools. Aquatic Living Resources 22:225-232.
- [21] ICES (2019) Ninth Workshop on the Development of Quantitative Assessment Methodologies based on LIFE-history traits, exploitation characteristics, and other relevant parameters for data-limited stocks (WKLIFE IX). ICES Scientific Reports 1:77.
- [22] ICES (2021) ICES Strategic Plan. ICES, International Council for the Exploration of the Sea.
- [23] ICES (2022) Workshop on ICES reference points (WKREF1). ICES Scientific Reports 4:2. ICES, Copenhagen. <http://doi.org/10.17895/ices.pub.9822>
- [24] ICES (2023) Guide to ICES advisory framework and principles. In: Report of the ICES Advisory Committee, 2023. ICES Advice 2023, section 1.1.
- [25] ICES (2024) Benchmark workshop on horse mackerel and boarfish (WKBHMB). ICES Scientific Reports. 6:8. 296 pp. <https://doi.org/10.17895/ices.pub.2500>
- [26] ICES (2025) Horse mackerel (*Trachurus trachurus*) in Division 9.a (Atlantic Iberian waters). ICES Stock Annexes.
- [27] ICES (2025) Working Group on Southern Horse Mackerel, Anchovy, and Sardine (WGHANSA). ICES Scientific Reports 7:70. ICES, Copenhagen.
- [28] ICES (2025) Horse mackerel (*Trachurus trachurus*) in Division 9.a (Atlantic Iberian waters). ICES Stock Annexes 22.
- [29] IUCN (2025) The IUCN Red List of Threatened Species. Version 2025-2 (Global). <https://www.iucnredlist.org/>. Accessed 2025.
- [30] Johnston SJ, Butterworth DS (2005) The South African horse mackerel assessment using an age-structured production model, with future biomass projections. MARAM, Department of Mathematics and Applied Mathematics, University of Cape Town, Rondebosch.
- [31] Kell LT, Mosqueira I, Grosjean P, Fromentin J-M, Garcia D, Hillary R, Jardim E, Mardle S, Pastoors MA, Poos JJ, Scott F, Scott RD (2007) FLR: an open-source framework for the evaluation and development of management strategies. ICES Journal of Marine Science 64:640-646.
- [32] Kilduff P, Carmichael J, Latour R (2009) Guide to Fisheries Science and Stock Assessments. Atlantic States Marine Fisheries Commission, Washington DC.
- [33] Lee H-H, Maunder MN, Piner KR, Methot RD (2012) Can steepness of the stock-recruitment relationship be estimated in fishery stock assessment models? Fisheries Research 125-126:254-261.

- [34] Ly B, Diop M, Girardin M (1996) Guide et nomenclature nationale commerciale des espèces marines (poissons, crustacés et mollusques) pêchées en Mauritanie. Centre National de Recherches Océanographiques et des Pêches, Ministère des Pêches et de l'Économie Maritime.
- [35] Mace PM, Doonan IJ (1988) A generalized bioeconomic simulation model for fish stock assessment. New Zealand Fisheries Assessment Research Document.
- [36] Maunder MN (2012) Evaluating the stock-recruitment relationship and management reference points: Application to summer flounder (*Paralichthys dentatus*) in the U.S. mid-Atlantic. *Fisheries Research* 125-126.
- [37] Maunder MN, Punt AE (2013) A review of integrated analysis in fisheries stock assessment. *Fisheries Research* 142:61-74.
- [38] Methot RD Jr, Wetzel CR (2013) Stock synthesis: A biological and statistical framework for fish stock assessment and fishery management. *Fisheries Research* 142:86-99.
- [39] Meyer R, Millar RB (1999) Bayesian stock assessment using a state-space implementation of the delay difference model. *Canadian Journal of Fisheries and Aquatic Sciences* 56:37-52.
- [40] Miller, T. J., and Brooks, E. N. (2021). Steepness is a slippery slope. *Fish and Fisheries*, 22(3), 634-645.
- [41] Murua H, Saborido-Rey F (2003) Female reproductive strategies of marine fish species of the North Atlantic. *Journal of Northwest Atlantic Fishery Science* 33:23-31.
- [42] Myers RA, Hutchings JA, Barrowman NJ (1997) Why do fish stocks collapse? The example of cod in Atlantic Canada. *Ecological Applications* 7:91-106.
- [43] Myers RA (2001) Stock and recruitment: generalizations about maximum reproductive rate, density dependence, and variability using meta-analytic approaches. *ICES Journal of Marine Science* 58:937-951.
- [44] Needle CL, O'Brien CM, Darby CD, Smith MT (2003) Incorporating time-series structure in medium-term recruitment projections. *Scientia Marina* 67(Suppl. 1):201-209. <https://doi.org/10.3989/scimar.2003.67s1201>
- [45] Nogueira Gassent A (2017) Changes in the overexploited demersal fish assemblages in the Northwest Atlantic: the Southern Grand Banks and the Flemish Cap. Tesis, Universidade de Vigo.
- [46] Pope JG (1972) An investigation of the accuracy of virtual population analysis using cohort analysis. *Research Bulletin of the International Commission for the Northwest Atlantic Fisheries* 9:65-74.
- [47] Puente RH, Costas G, Mendes H, Cebrián JL, Nogueira A (2026) Analysis of the stock-recruitment relationship for the southern horse mackerel (*Trachurus trachurus*) stock in the ICES Division 27.9.a. Working Document 01-WGHANSA-1, Working Group on Southern Horse Mackerel, Anchovy and Sardine (WGHANSA), online meeting, 25-28 May 2026.
- [48] Punt AE, Hilborn R (1997) Fisheries stock assessment and decision analysis: the Bayesian approach. *Reviews in Fish Biology and Fisheries* 7:35-63.
- [49] Punt AE, Dorn MW (2014) Comparisons of meta-analytic methods for deriving a probability distribution for the steepness of the stock-recruitment relationship. *Fisheries Research* 149:43-54.
- [50] Quinn TJ, Deriso RB (1999) *Quantitative Fish Dynamics*. Oxford University Press, New York.

- [51] Reid PC, Borges MF, Svendsen E (2001) A regime shift in the North Sea circa 1988 linked to changes in the North Sea horse mackerel fishery. *Fisheries Research* 50:163-171.
- [52] Ricker WE (1954) Stock and recruitment. *Journal of the Fisheries Research Board of Canada* 11:559-623.
- [53] Ricker WE (1975) Computation and interpretation of biological statistics of fish populations. *Bulletin of the Fisheries Research Board of Canada* 191:1-382.
- [54] Rodionov SN (2005) A brief overview of the regime shift detection methods. Large-scale disturbances (regime shifts) and recovery in aquatic ecosystems: challenges for management toward sustainability, 17-24.
- [55] Romero P (2002) An etymological dictionary of taxonomy. Madrid, unpublished.
- [56] Rose GA (2003) Fisheries Resources and Science in Newfoundland and Labrador: An Independent Assessment. Royal Commission on Renewing and Strengthening Our Place in Canada, St. John's, Newfoundland and Labrador.
- [57] Russ GR, Zeller DC (2003) From mare liberum to mare reservarum. *Marine Policy* 27:75-78.
- [58] Schaefer MB (1954) Some aspects of the dynamics of populations important to the management of commercial marine fisheries. *Inter-American Tropical Tuna Commission Bulletin* 1:27-56.
- [59] Schnute J (1985) A general theory for analysis of catch and effort data. *Canadian Journal of Fisheries and Aquatic Sciences* 42:414-429.
- [60] Silvar-Viladomiu P, Batts L, Minto C, Miller D, Lordan C (2024) An empirical review of ICES reference points. *ICES Journal of Marine Science* 81:1201-1214.
- [61] Skalski JR, Ryding KE, Millspaugh JJ (2010) *Wildlife Demography: Analysis of Sex, Age, and Count Data*. Elsevier, Burlington, MA.
- [62] Smith-Vaniz WF (1986) Carangidae. In: Whitehead PJP, Bauchot M-L, Hureau J-C, Nielsen J, Tortonese E (ed) *Fishes of the north-eastern Atlantic and the Mediterranean*, vol 2. UNESCO, Paris, pp 815-844.
- [63] Subbey S, Devine JA, Schaarschmidt U, Nash RDM (2014) Modelling and forecasting stock-recruitment: current and future perspectives. *ICES Journal of Marine Science* 71:2307-2322.
- [64] United Nations (2002) *Johannesburg Plan of Implementation*. World Summit on Sustainable Development, Johannesburg.
- [65] United Nations (1982) *United Nations Convention on the Law of the Sea*. 1833 U.N.T.S. 397.
- [66] Yang Y, Yamakawa T (2022) Re-examination of stock-recruitment relationships: a meta-analysis. *ICES Journal of Marine Science* 79:1380-1393.
- [67] Walters C, Maguire J-J (1996) Lessons for stock assessment from the northern cod collapse. *Reviews in Fish Biology and Fisheries* 6:125-137.
- [68] Winker H, Cardinale M, Gerritsen H, Gil Herrera J, Castellanos P, Farias I, Sampedro P, Moura T, Mosqueira I, Kell L (2025) The ICES MSY approach to reference point estimation is not precautionary. *ICES Journal of Marine Science*.